NASA TECHNICAL NOTE

NASA TN D-4315

NASA TN D-4315

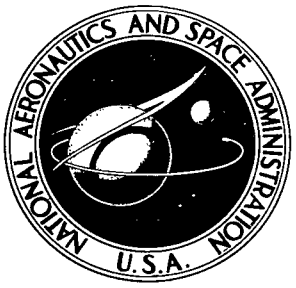

PRELIMINARY CONSIDERATIONS FOR FAST-SPECTRUM, LIQUID-METAL COOLED NUCLEAR REACTOR PROGRAM FOR SPACE-POWER APPLICATIONS

by Gerald P. Lahti, Edward Lantz, and John V. Miller

Lewis Research Center
Cleveland, Ohio

NATIONAL AERONAUTICS AND SPACE ADMINISTRATION • WASHINGTON, D. C. • MARCH 1968

PRELIMINARY CONSIDERATIONS FOR FAST-SPECTRUM, LIQUID-METAL COOLED NUCLEAR REACTOR PROGRAM FOR SPACE-POWER APPLICATIONS

By Gerald P. Lahti, Edward Lantz, and John V. Miller

Lewis Research Center
Cleveland, Ohio

NATIONAL AERONAUTICS AND SPACE ADMINISTRATION

For sale by the Clearinghouse for Federal Scientific and Technical Information
Springfield, Virginia 22151 – CFSTI price $3.00

PRELIMINARY CONSIDERATIONS FOR FAST-SPECTRUM, LIQUID-METAL COOLED NUCLEAR REACTOR PROGRAM FOR SPACE-POWER APPLICATIONS

by Gerald P. Lahti, Edward Lantz, and John V. Miller

Lewis Research Center

SUMMARY

A nuclear reactor suitable for space-power applications should ideally be compact, light weight, easily controlled, and be capable of operation for a substantial period of time with little or no maintenance. In order to develope a reliable nuclear reactor for space power, however, it may be necessary to compromise some of these requirements to some degree due to other considerations such as shielding requirements which may be necessary to protect personnel and equipment.

To identify and evaluate the relative importance of some of these parameters, a preliminary study was made in which reactor size and shield weight requirements were calculated for several compositions of uranium nitride and uranium dioxide (UN and UO_2) fuel materials under various operating conditions. A fast-spectrum, lithium-cooled reactor was selected for the study since it potentially will result in the smallest reactor that is capable of operating at the required temperature levels. In order to determine man-rated shielding requirements, a 2-millirem-per-hour radiation dose at 66 feet (20 m) was selected as a reasonable value, being of the same order of magnitude as that which would be received from galactic cosmic rays in interplanetary space.

For the relatively small reactors considered in this study, nuclear criticality and the allowable fuel burnup limits essentially determine the required reactor size and resulting weight of the shielding. The importance of the other variables, such as allowable steady-state heat-transfer limits, coolant temperatures and flow rates, coolant hole sizes, etc., is only secondary in determining the weight of the reactor plus shield. Choice of the proper value for each of these parameters can be based on overall system performance, availability of design data, material limitations, and manufacturing feasibility.

From the results of this preliminary study, it appears that nuclear stability and control, fuel material development, and shielding optimization are areas in which additional work must be performed to develop a reliable nuclear reactor system for space-power application.

INTRODUCTION

Nuclear reactors are being considered as the potential heat source for many space-power applications. These include auxiliary electric power generation using Rankine (ref. 1), Brayton (ref. 2), or thermionic systems (ref. 3). In addition, space propulsion devices which utilize electrical energy, such as ion engines or electric-arc jets, require a substantial source of energy which could also be obtained from a nuclear reactor (refs. 4 and 5).

A nuclear reactor suitable for space-power application should ideally be compact, lightweight, and easily controlled. It should also be capable of sustained operation at a relatively high temperature and power level with little or no maintenance. Many of these requirements will obviously be hard to achieve, particularly if it is necessary to surround the reactor with heavy biological shielding to protect personnel and equipment. In order to develop a reliable nuclear reactor for space power, therefore, it may be necessary to compromise many of the ideal requirements to some degree and optimize the system based on the more important considerations.

To ascertain the applicability of nuclear reactors to the various systems, Lewis Research Center has undertaken a program of investigation. The preliminary phase of this investigation, which is summarized in this report, has been concerned with the identification of areas where additional technological information would be required to design and construct a reliable operating reactor for space-power systems. Having identified such problem areas, an experimental and analytical research program can be initiated to obtain the required data. Programs in the area of the overall system development (i.e., thermionic, Brayton, and Rankine systems) are currently being conducted. The establishment of a broad base of knowledge in both reactor and energy conversion technology should facilitate the development of nuclear electric power systems for space applications.

BASIC ASSUMPTIONS

The use of a man-rated nuclear reactor for space applications will require a significant amount of biological shielding to limit the radiation dose from the reactor. The shielding requirements may vary from one direction to another but, nevertheless, the need for shielding does indicate a need for a minimum size reactor if low system weights are to be achieved.

For this reason, a fast-spectrum, liquid-metal cooled reactor was selected for study since it seems to offer the greatest potential for minimum weight systems. Complete (4π) shielding was included in the study. An allowable dose rate of 2 millirems per hour to a man at a distance of 66 feet (20 m) was selected as a design goal. Lithium was chosen as

the reactor coolant because of its excellent thermal properties and low vapor pressure in the temperature range of possible interest.

For small, high performance reactors, the conductivity of the fuel material is of great importance in reducing the temperature in the fuel. Since low fuel temperatures are desirable for structural considerations and fission product retention, cermet fuels were therefore selected as the potential fuel because of their greater strength and increased thermal conductivity. At the temperature of interest, matrix metals would be limited to tungsten, molybdenum, tantalum, and their alloys. Both uranium nitride and uranium dioxide (UN and UO_2) were considered as the possible dispersion fuel material.

The operating life requirement for the reactor was set at 20 000 hours at full power. Maximum usable reactor outlet temperature was assumed to be 3000° R (1670° K) based on reactor structural material strengths and reasonably achievable operating turbine temperatures for Rankine and Brayton Systems (ref. 1 and 2). With lithium as the coolant, it is possible to operate at a reactor outlet coolant pressure of less than 50 psi (34.5 N/cm^2) without encountering steady-state boiling. This low pressure is an important factor since it determines structural material thickness and hence thermal stresses in the pressure vessel, piping, and other components containing the coolant and subjected to gamma heating.

The cylindrical reactor core was cooled by the axial flow of lithium through uniformly spaced holes piercing the fuel cermet in a triangular array. Each of the holes is clad by unfueled structural material 0.010 inch (0.25 mm) thick. The fuel cermet was considered to have a basic average composition of 45 percent fuel, 45 percent metal matrix, and 10 percent void. Higher fuel loadings will be required in parts of the core to flatten radial and axial power distribution. The 10 percent void fraction included in the cermet was considered the minimum void fraction required to achieve containment of fission gases released from the fuel. The maximum temperature in the cermet fuel was limited to 3500° R (1945° K) in order to restrict the temperature gradients to values which appear to be operationally feasible for tungsten-UO_2 cermets (ref. 6).

Although the power requirements of the various space power systems are quite different, the investigation was generally conducted on a reactor with a thermal output of 2.5 megawatts, which, assuming a conversion efficiency of 20 percent, could produce 500 kilowatts of useful electric power. Perturbations about this power level were also conducted to determine the effect of reactor power on the weight of the system. Axial and radial peak-to-average power factors of 1.20 and 1.10, respectively, were assumed, and an excess multiplication factor Δk of 10 percent was used in the criticality calculations to allow sufficient reactivity for power flattening, temperature defect, fuel depletion, and other nuclear contingencies.

TABLE I. - NEUTRON ENERGY GROUPS USED FOR NEUTRONIC ANALYSIS

Group	Neutron energy range	
	eV	J
1	3.68×10^{6} to 14.9×10^{6}	5.89×10^{-13} to 2.39×10^{-12}
2	2.23×10^{6} to 3.68×10^{6}	3.57×10^{-13} to 5.89×10^{-13}
3	1.35×10^{6} to 2.23×10^{6}	2.17×10^{-13} to 3.57×10^{-13}
4	8.21×10^{5} to 1.35×10^{6}	1.32×10^{-13} to 2.17×10^{-13}
5	4.98×10^{5} to 8.21×10^{5}	7.98×10^{-14} to 1.32×10^{-13}
6	3.02×10^{5} to 4.98×10^{5}	4.84×10^{-14} to 7.98×10^{-14}
7	1.83×10^{5} to 3.02×10^{5}	2.93×10^{-14} to 4.84×10^{-14}
8	1.11×10^{5} to 1.83×10^{5}	1.78×10^{-14} to 2.93×10^{-14}
9	4.08×10^{4} to 1.11×10^{5}	6.54×10^{-15} to 1.78×10^{-14}
10	1.50×10^{4} to 4.08×10^{4}	2.40×10^{-15} to 6.54×10^{-15}
11	5.53×10^{3} to 1.50×10^{4}	8.86×10^{-16} to 2.40×10^{-15}
12	7.49×10^{2} to 5.53×10^{3}	1.20×10^{-16} to 8.86×10^{-16}
13	.414 to 7.49×10^{2}	6.63×10^{-20} to 1.20×10^{-16}

NEUTRONIC CALCULATIONS

Verification of Calculational Procedures

Before the fast, liquid-metal cooled reactors were analyzed, neutronic calculations were performed for several tungsten reflected, pure fuel, spherical, critical experiments (refs. 7 and 8) to verify the cross sections of the principal materials and the general analytical procedure. For these calculations, the discrete angle, multienergy group, neutron transport program TDSN was used (ref. 9). The P_1 approximation for neutron scattering and S_4 discrete angle segmentation were used.

Multigroup cross sections used in the analysis were obtained from the GAM II program (ref. 10) which averaged the cross sections over the slowing down spectrum. Separate GAM II calculations were performed for the homogenized core and reflector materials using the 13 neutron energy groups shown in table I. The lower energy of the lowest group used was 0.414 eV (0.663×10^{-19} J); in these tungsten reflected fast reactors, the number of neutrons with energy less than 0.414 electron volt is negligible.

Results of the calculations performed for the two most pertinent critical experiments are shown in table II which shows that the calculated multiplication factors (k_{eff}) for these critical spheres are about 2 percent higher than the experimental value of 1.00.

After verifying the basic calculational procedure on the spherical critical experiments, the next step in the analysis of the neutronic behavior of a fast, liquid-metal

TABLE II. - CALCULATION OF SPHERICAL GEOMETRY CRITICAL EXPERIMENTS

Core					Reflector					Reference	Calculated, k_{eff}
Material	Density		Diameter		Material	Density		Thickness			
	g/cm^3	$lb/in.^3$	cm	in.		g/cm^3	lb/in.	cm	in.		
Oralloy[a]	18.8	0.679	12.822	5.048	Tungsten[b]	17.39	0.628	10.16	4.00	2	1.018
Uranium 233[c]	18.62	.672	9.200	3.622	Tungsten[d]	17.2	.621	5.790	2.279	3	1.023

[a] 93.5 percent U^{235}, 6.5 percent U^{238}.
[b] 7 wt. % Ni and 3 wt. % Cu.
[c] 1.1 wt. % U^{234} and 0.7 wt. % U^{238}.
[d] 5.5 wt. % Ni, 2.5 wt. % Cu, and 0.7 wt. % Zr.

cooled reactor was to determine the multiplication factors and power distributions for cylindrical reactors of the same basic materials; that is, U^{233} and U^{235} fuel and tungsten. (The two-dimensional, cylindrical geometry option of the TDSN program had been previously verified by using the Lewis ZPR-I and ZPR-II critical experiments (ref. 11).) If the same 13 neutron energy group cross sections used in the spherical calculations were used in a two-dimensional cylindrical geometry analysis, it would be expected that the results would have about the same accuracy (+2 percent) in the determination of k_{eff}. The use of 13-group, P_1 cross sections in a two-dimensional calculation for a parametric survey, however, would require considerable computer time. Therefore, a comparative study was performed to evaluate the accuracy of a 13-group, P_1, one-dimensional procedure which was used in calculating the cylindrical reactors of this survey.

This was accomplished in two steps. First, a one-dimensional radial calculation with 13-group, P_1 cross sections was compared with the results obtained with an identical calculation using six-group, P_0 cross sections. Secondly, a two-dimensional, six-group, P_0 calculation was made to determine the difference between the one- and two-dimensional six-group, P_0 results. The multiplication factor determined with the one-dimensional, six-group calculation was 0.6 percent greater than that of the corresponding 13-group solution. Between the two-dimensional and one-dimensional, six-group results, the difference in using one-dimensional calculation was 0.8 percent greater. Neither of these differences are significant, particularly since the parametric study was meant to yield relative rather than absolute results.

The two-dimensional, six-group, P_0 calculation was also used as the basis for determining the reflector savings of 4-inch (10.16-cm) axial reflectors, which were assumed to be composed of 85-percent tungsten and 15-percent lithium 7 by volume. By varying the transverse buckling in a one-dimensional radial calculation, the equivalent axial reflector savings was calculated to be 8.5 centimeters.

Results of Parametric Survey

Using the method described, a parametric survey of the fast spectrum, liquid-metal cooled reactor was performed. All the cores of this survey had a 4-inch (10.16-cm) thick radial reflector which was composed of 95-volume-percent tungsten and 5-volume-percent lithium 7. As previously mentioned, the axial reflectors were 4 inches (10.16 cm) thick and composed of 85-percent tungsten and 15-percent lithium 7.

Figure 1 shows the required core diameter D as a function of the volume fraction of lithium 7 coolant for an effective neutron multiplication factor k_{eff} of 1.10. Specific calculations were performed for coolant fractions of 10, 20, and 35 volume percent using three different fuel materials, $U^{235}O_2$, $U^{233}O_2$, and $U^{233}N$. The previously assumed matrix composition of 45 percent fuel, 45 percent tungsten, and 10 percent void was used in the calculations with the density of the UO_2 and UN fuel taken as 0.39 and 0.49 pounds per cubic inch (10.7 and 13.5 g/cm^3), respectively. Although the general shape of the curves in figure 1 are identical, the use of U^{233} instead of U^{235} or, the use of UN rather than UO_2, can decrease the size requirements of the reactor, based on neutronic considerations only. For example, at a coolant fraction of 10 percent, the required length and diameter (L/D = 1) of the $U^{233}N$, $U^{233}O_2$, and $U^{235}O_2$ reactors, excluding reflector thicknesses, are 8.6, 10.5, and 17.4 inches (21.8, 26.7, and 44.3 cm), respectively.

In addition to determining the effect of coolant fraction and fuel material on the required reactor size (fig. 1), calculations were performed to determine the effect of

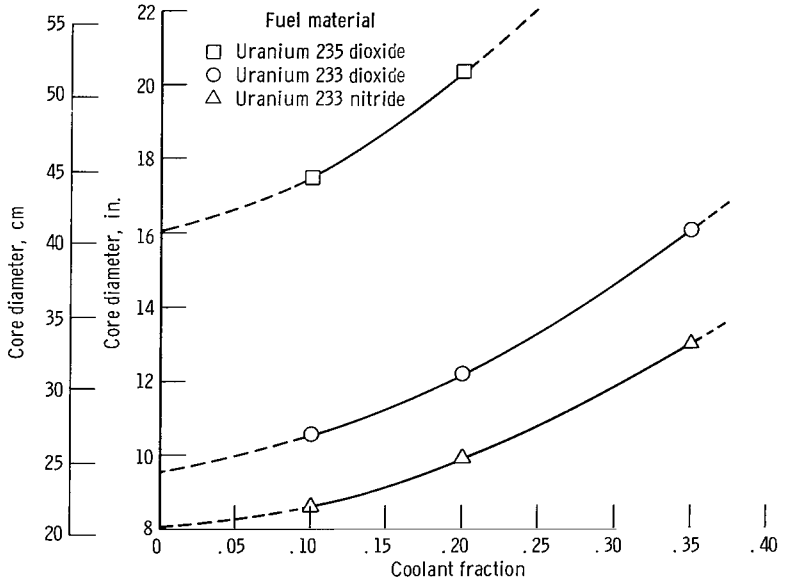

Figure 1. - Effect of fuel and coolant fraction on core size. Effective multiplication factor, 1.10; reactor length-to-diameter ratio, 1.0; coolant, lithium 7. Fuel matrix composition: fuel, 45 volume percent; void, 10 volume percent; tungsten, 45 volume percent.

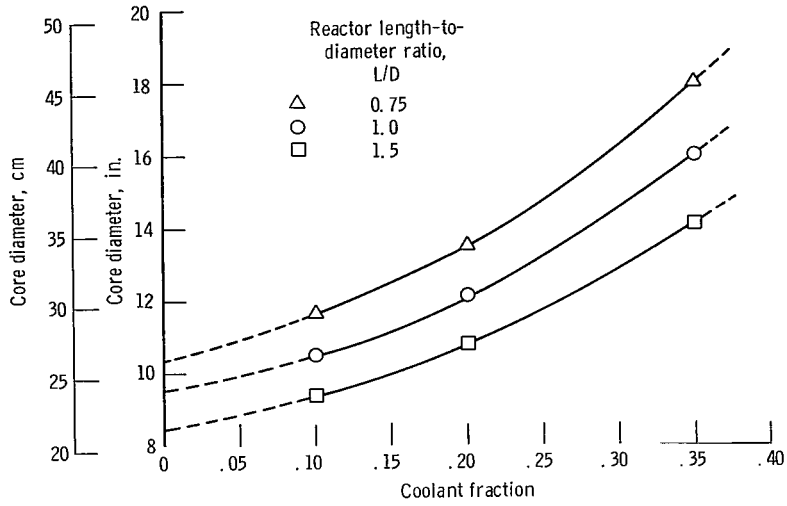

Figure 2. - Effect of reactor length-to-diameter ratio and core coolant fraction on core size. Effective multiplication factor, 1.10; fuel, uranium 233 dioxide; coolant, lithium 7. Fuel-matrix composition: fuel, 45 volume percent; tungsten, 45 volume percent; void, 10 volume percent.

changing the core length-to-diameter ratio and the effect of changing the fuel matrix composition. Figure 2 shows the results for the first of these additional studies; required core diameters for length-to-diameter ratios of 0.75 and 1.5 are compared with the previous value (L/D = 1) for the $U^{233}O_2$ fueled reactor. The required core diameter decreases monotonically with increasing length-to-diameter ratio of the reactor. At a coolant fraction of 10 percent, for example, the required core diameters are 11.6, 10.5, and 9.4 inches (29.5, 26.7, and 23.9 cm), for L/D ratios of 0.75, 1.0, and 1.5, respectively. If only frontal shadow shielding were required, the small frontal area (i.e., smaller diameter) of the longer cores could reduce the weight-to-power ratio of the reactor and radiation shield.

The results of varying fuel composition are shown on figure 3 where the required core diameter (L/D = 1) necessary to maintain a 1.10 multiplication factor is shown for three different $U^{233}N$ fuel compositions. Table III lists the composition and resulting size requirements for the three cases at a coolant fraction of 10 percent. The required core diameters for the conditions shown give an indication of the reduction in core size that may be possible if higher fuel loadings are shown to be feasible.

Another possible use of increased fuel loadings would be to reduce the percentage of fuel burnup. Fuel burnup is important in the neutronic design of the reactor since the amount of fuel depleted over the lifetime of the reactor will affect the excess reactivity requirements of the core. For the fast-spectrum reactors considered in this study, approximately 1-percent excess reactivity will be required for each 2-percent fuel depletion.

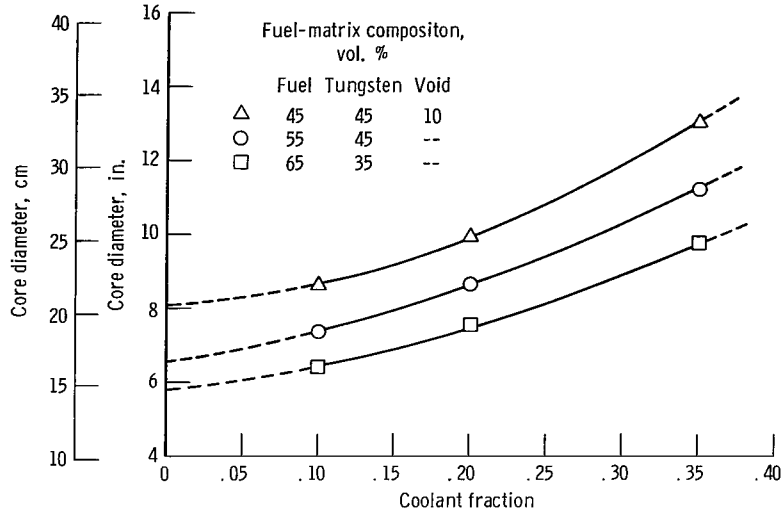

Figure 3. - Effect of fuel-matrix composition and core coolant fraction on core size. Effective multiplication factor, 1.10; fuel, uranium 233 nitride; coolant, lithium 7.

TABLE III. - EFFECT OF FUEL COMPOSITION ON REQUIRED CORE SIZE

[k_{eff}, 1.10; length to diameter ratio, 1; coolant fraction, 10 volume percent.]

Case	Fuel-matrix composition, vol. %			Required core diameter		Relative fuel burnup[a]
	$U^{233}N$	Tungsten	Void	in.	cm	
1	45	45	10	8.6	21.8	1.0
2	55	45	--	7.4	18.8	1.28
3	65	35	--	6.4	16.3	1.68

[a]Relative to the 45-45-10 vol. % composition.

Fuel burnup is also important to the integrity of the fuel elements because of the internal burnup of fission products and fuel swelling related to the total fuel depletion. The exact mechanism by which fuel swelling occurs is not yet clearly understood; in cermet fuels, for example, the role of the matrix material in suppressing fuel swelling has not been established. As used in this report, the term "percentage of fuel burnup" refers to the percent of uranium depleted from the total uranium originally contained in the core. Because the intent of the parametric survey was to show relative variations, this definition will suffice even though the percentage of uranium depleted from the fuel-tungsten matrix may actually be the more important parameter.

Obviously, if the fuel loading is increased for a given reactor size and configuration,

TABLE IV. - EFFECT OF FUEL COMPOSITION ON FUEL BURNUP FOR A GIVEN CORE SIZE

[Core diameter, 8.6 inches (21.8 cm); length to diameter ratio, 1.0.]

Case	Fuel-matrix composition, vol. %			Required coolant fraction[a]	Relative fuel burnup[b]
	$U^{233}N$	Tungsten	Void		
1	45	45	10	0.10	1.0
2	55	45	--	.20	.970
3	65	35	--	.283	.969

[a]To maintain $k_{eff} = 1.10$.

[b]Relative to 45-45-10 vol. % fuel composition.

the fuel burnup will decrease proportionally for the same operating conditions. However, adding more fuel to a given size core would also increase the excess reactivity of the reactor and sufficient reactivity control must be available. If the reactor size were merely decreased to accommodate the increased fuel loading, the relative fuel burnup of the smaller, higher loaded cores would increase significantly (table III). It is possible, however, to obtain a reduction in fuel burnup by increasing fuel loading and without increasing the excess reactivity of the reactor. This can be accomplished by adjusting the coolant fraction to maintain the same reactivity margin. Table IV shows the comparative fuel burnup for three 8.6-inch (21.8-cm) reactors using the fuel compositions from figure 3. Only a relatively small reduction (3 percent) in fuel burnup is achieved in this manner.

Another and somewhat trivial method by which fuel burnup could be reduced without changing the coolant fraction or increasing excess reactivity would be to replace some of the tungsten matrix with U^{238}, a less fissionable isotope of uranium. By diluting the fuel in this manner, the percentage of fuel depleted from the uranium is reduced by the amount of diluent added. However, since the U^{238} replaced a much stronger matrix material (i.e., tungsten), it is not clear that this method would actually result in a net gain insofar as the structural integrity of the fuel element is concerned.

Reactor, Stability, and Control

Since the delayed neutron fraction for U^{233} is only about 0.4 that of U^{235}, there is a question on the control and power stability of the smaller (U^{233}) reactors. Because of the smaller delayed neutron fraction, the U^{233} cores will, in general, require more precise reactivity control, and the rate of positive reactivity insertion will have to be more limited. At present, it is not known whether the Doppler coefficient, which is useful for

control and termination of a reactivity excursion, is positive or negative for U^{233}. It is known that, in similar reactors, with a median fission energy of about 0.5 MeV (8×10^{-13} J), the Doppler coefficient of pure U^{235} is positive, but of very small magnitude (ref. 12). In this reactor, the calculated Doppler coefficient of tungsten is negative, and an order of magnitude greater than that of the positive U^{235} fuel coefficient. As a result, the effect of the tungsten would completely override the positive fuel coefficient. It appears that a similar situation may occur for a reactor fueled with U^{233}. However, detailed control and stability studies such as outlined in references 13 and 14, will have to be made, and if necessary, a negative reactivity temperature coefficient may have to be engineered into the design of a fast-spectrum, tungsten U^{233} reactor. An example of an engineered expansion approach is given in reference 15, and there are other approaches that may be practical.

SHIELDING ANALYSIS

One of the major considerations in a general parametric study of a nuclear reactor for space-power applications is the shielding requirements which may be imposed on the system for a particular mission. For an unmanned mission, for example, a simple shadow-shield to protect equipment and instrumentation may be sufficient. Conversely, a manned mission may require biological shielding in all directions to protect personnel as well as equipment.

Obviously, the weight of any reactor system will depend on the extent to which such shielding requirements are imposed and on the allowable dose rate which is deemed tolerable. The most conservative approach would be to determine the shield configuration and weight for the case where complete biological shielding is required in all directions, realizing that a significant savings in weight would result if this requirement were not necessary. In this study, the conservative approach was used. A biological shield configuration for a reactor producing 2.5 megawatts of thermal power (MW_t) was determined which would limit the dose received by a man from reactor radiation sources to 2 millirem per hour at a point 66 feet (20 m) in any direction from the center of core. At this dose rate, the crew would receive 20 rem per year from reactor radiation. This radiation dose compares with the 30 to 100 rem per year background radiation from galactic cosmic rays which would be received in interplanetary space.

To facilitate computation, one-dimensional transport calculations were performed in which the reactor was represented by an equivalent sphere with a diameter equal to the length of the diagonal of the right circular cylinder. This, for example, requires that a 10-inch (25.4-cm) cylindrical reactor (L/D = 1) be represented by a sphere having a 14.14-inch (35.9-cm) diameter. Although the volumes of the cylinder and sphere are

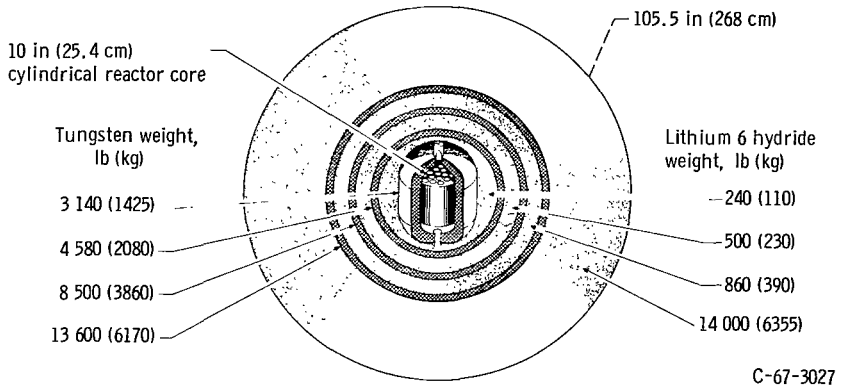

Figure 4. - Multilayered tungsten - lithium 6 hydride shield. Total weight, 46 080 pounds (20 920 kg).

not the same, the gamma and neutron leakage from the sphere will not be appreciably different (except in the immediate vicinity of the corners of the cylinder) from that of the cylinder. Since an actual reactor will require flow distribution plenums, support structures, etc., the apparent increase in volume is not unrealistic.

The remainder of the core-reflector-shield configuration (fig. 4) consisted of a series of spherical shells arranged concentrically about the tungsten-$U^{233}O_2$ reactor core. A 4-inch (10.16-cm) thick reflector surrounds the core and is followed by a 0.35-inch (0.9-cm) pressure vessel and then by alternate layers of lithium 6 hydride (Li^6H) and tungsten which comprise the basic shielding materials used in this analysis. Table V lists the composition of each region.

The GAM II computer program (ref. 10) was used to obtain a set of neutron microscopic cross sections for the elements used in the reactor-shield configuration. Computations were made using P_1 scattering cross sections and a resonance calculation for tungsten. Broad group neutron cross sections were evaluated for 13 fast energy groups, and a single group thermal cross section was obtained using the GATHER II computer

TABLE V. - AVERAGE COMPOSITION OF VARIOUS REGIONS USED IN SHIELDING ANALYSIS

Material	Hydrogen		Lithium 6		Lithium 7		Oxygen		Tungsten		Uranium		Total	
	Density													
	lb/ft^3	g/cm^3	lb/ft^3	g/cm^3	lb/ft^3	g/cm^3	lb/ft^3	g/cm^3	lb/ft^3	g/cm^3	lb/ft^3	g/cm^3	lb/ft^3	g/cm^3
Core	0	0	0	0	3.37	0.054	31.3	0.502	511.0	8.2	226.0	3.62	772	12.38
Reflector	0	0	0	0	1.68	.027	0	0	1145.0	18.34	0	0	1147	18.37
Lithium-6 hydride shield	6.67	.107	40.0	.643	0	0	0	0	0	0	0	0	46.7	.75
Tungsten shield	0	0	0	0	0	0	0	0	1205	19.3	0	0	1205	19.3

TABLE VI. - NEUTRON ENERGY GROUPS USED IN

SHIELDING ANALYSIS

Group	Neutron energy range					
	eV			J		
1	6.07×10^{6}	to	14.9×10^{6}	9.72×10^{-13}	to	2.39×10^{-12}
2	3.68×10^{6}	to	6.07×10^{6}	5.89×10^{-13}	to	9.72×10^{-13}
3	2.23×10^{6}	to	3.68×10^{6}	3.57×10^{-13}	to	5.89×10^{-13}
4	1.35×10^{6}	to	2.23×10^{6}	2.17×10^{-13}	to	3.57×10^{-13}
5	8.20×10^{5}	to	1.35×10^{6}	1.32×10^{-13}	to	2.17×10^{-13}
6	4.98×10^{5}	to	8.20×10^{5}	7.98×10^{-14}	to	1.32×10^{-13}
7	1.83×10^{5}	to	4.98×10^{5}	2.93×10^{-14}	to	7.98×10^{-14}
8	6.70×10^{4}	to	1.83×10^{5}	1.07×10^{-14}	to	2.93×10^{-14}
9	9.10×10^{3}	to	6.70×10^{4}	1.45×10^{-15}	to	1.07×10^{-14}
10	4.54×10^{2}	to	9.10×10^{3}	7.27×10^{-17}	to	1.45×10^{-15}
11	6.14×10^{1}	to	4.54×10^{2}	9.84×10^{-18}	to	7.27×10^{-17}
12	3.06×10^{0}	to	6.14×10^{1}	4.90×10^{-19}	to	9.84×10^{-18}
13	4.14×10^{-1}	to	3.06×10^{0}	6.63×10^{-20}	to	4.90×10^{-19}
14	0	to	4.14×10^{-1}	0	to	6.63×10^{-20}

program (ref. 16). The neutron energy groups used in the calculations are shown in table VI.

The one-dimensional S_n neutron transport code DTF IV (ref. 17) with S_{12} gauss quadrature was used with the GAM II/GATHER II cross sections to obtain the neutron flux distribution throughout the reactor-reflector-shield assembly. With this neutron flux distribution and a knowledge of the neutron interactions which produce secondary gamma rays, the number and spatial distribution of secondary gamma-producing events in the shield and core reflector were calculated. This information, along with the gamma spectrum associated with each event (ref. 18), was used to determine the distribution of secondary gamma sources throughout the shield. Calculations were then made to evaluate the secondary gamma dose from the sources, the neutron dose, and the primary gamma dose from core gamma sources using a point-kernel, line-of-sight program, QADP5A. This computer code is a modified version of the Los Alamos Laboratory program QAD4 (ref. 19) and uses infinite-medium buildup factors for gammas and the Albert-Welton dose kernel to estimate the fast neutron dose.

SHIELD WEIGHT REQUIREMENTS

If only the neutrons and gamma rays leaving the unreflected reactor are considered, a biological shield consisting of 6.6 inches (16.8 cm) of tungsten followed by 39 inches (99 cm) of Li^6H is sufficient to limit the dose rate of a 10-inch (25.4-cm), 2.5-MW_t reactor to 2 millirem per hour at a point 66 feet (20 m) from the center of the core. The

weight of this configuration is 23 200 pounds (10 540 kg). However, the neutrons leaking from the reactor interact with the shielding materials, particularly the tungsten, and produce secondary gamma rays. For this 23 200 pound (10 540 kg) shield configuration, the secondary gammas generated throughout the shield result in a dose rate of about 20 000 millirem per hour at the dose detector point.

The Li^6 atom, with a high absorption cross section, captures neutrons, but emits alpha particles instead of gamma rays. Lithium 6 hydride is, therefore, a good secondary gamma suppressor as well as a good neutron absorber. However, if the order of the tungsten and Li^6H layers were merely reversed in the spherical shield design (i. e., the Li^6H located next to core and the tungsten on the outside), the dose rate at the detector would be reduced to the proper value, but the weight penalty incurred by moving the tungsten to the outer radius of the sphere would be 90 000 pounds (40 800 kg) as the total weight of this system is about 109 000 pounds (49 400 kg).

To reduce secondary gamma production without such a large weight increase, sections of the tungsten gamma shield are layered between sections of Li^6H. The resulting shield configuration using this layering technique for a 10-inch (25. 4-cm) diameter, 2. 5-MW_t reactor is shown on figure 4. This configuration limits the radiation dose from all reactor sources, including secondary gamma production, to the desired value (2 mrem/hr) at the detector point. The weight of this configuration (table VII) is 46 080 pounds

TABLE VII. - COMPOSITE SHIELD CONFIGURATION FOR 2. 5-MEGAWATTS THERMAL POWER, FAST SPECTRUM REACTOR

Region	Required thickness		Spherical outside diameter		Weight	
	in.	cm	in.	cm	lb	kg
Core[a]	-----	--	14. 14	36	660	300
Reflector[b]	4. 35	11	22. 8	58	3140	1425
Shield[c]						
Lithium 6 hydride	3. 94	10	30. 7	78	240	110
Tungsten	1. 97	5	34. 6	88	4580	2080
Lithium 6 hydride	3. 94	10	42. 5	108	500	230
Tungsten	1. 97	5	46. 5	118	8500	3860
Lithium 6 hydride	3. 94	10	54. 3	138	860	390
Tungsten	1. 97	5	58. 3	148	13 600	6170
Lithium 6 hydride	23. 6	60	105. 5	268	14 000	6355
					46 080	20 920

[a]10-in. (25. 4-cm) diam cylinder.
[b]Including pressure vessel.
[c]See fig. 4

(20 920 kg), or about twice the shield weight (23 200 lb) determined without consideration of secondary gamma production.

To demonstrate the effect of reactor size on shield weight, calculations were made over a range of core sizes. Neutron and gamma leakage from the reactor were assumed to be unaffected by a change in core size. The thickness of the tungsten reflector and the thickness and number of alternate layers of tungsten and Li^6H shielding were held constant as the core diameter changed. Figure 5 shows the resulting shield-plus-reactor weight for a 2.5 MW_t reactor for both the case in which the secondary gammas are considered and the case in which they are neglected. The weights calculated in this manner vary from 46 080 pounds (20 920 kg) from a 10-inch (25.4-cm) reactor to about 75 000 pounds (34 000 kg) for a 20-inch (50.8-cm) core. These weights estimates are based on the reactor and shield only. For a specific application in which full angular shielding is not required, the approximate weight of a particular shadow shield configuration having the

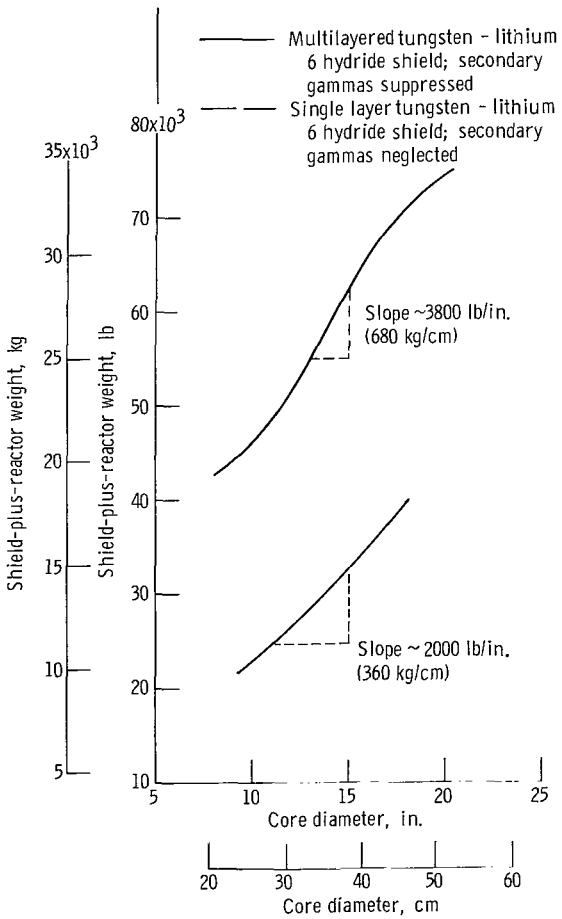

Figure 5. - Shield-plus-reactor weight for 2.5-megawatt thermal-power, fast-spectrum nuclear reactor.

same attenuation characteristics as the spherical (4π) shields presented in this study (fig. 5), may be estimated using the proportionality ratio of the solid angles of the shadow shield and the 4π-shield.

Another factor which can be easily estimated for the shield configuration considered here is a factor which accounts for changes in reactor power or the allowable dose at the detector point. From perturbation calculations, 0.4 inch (1 cm) of tungsten attenuates gamma rays by approximately a factor of 2, and 1.5 inches (3.8 cm) of Li^6H reduce the fast neutron dose by the same amount (i.e., a factor of 2).

If this additional material is conservatively added to the outermost spheres of the respective materials, the overall weight of the 10-inch (25.4-cm) reactor and shield is increased by 4500 pounds (2040 kg), or about a 10 percent increase in the weight. However, by distributing the additional tungsten and Li^6H throughout the shield, rather than lumping it into the outermost spheres, it might be possible to reduce the weight increase to perhaps 3000 pounds (1360 kg), or a 6 percent increase in overall weight. The 4500 pounds is a conservative estimate of the weight penalty caused by a factor of two change in reactor power, a factor of two change in the allowable dose rate, or a factor of two error in predicting radiation doses at the detector point, and it indicates that shield weight is rather insensitive to variations in these parameters.

The results presented in this analysis are preliminary in nature and must be refined by future shield optimization studies including the determination of the weight penalty imposed by cooling requirements of the shielding materials. Future calculations will also consider alternate shield materials and mixtures (dispersions) of materials as potential methods of decreasing the total shield weight. It would appear, however, that, even with shield optimization, additional weight savings of only 5 to 15 percent will be attained unless greatly relaxed dose constraint in certain directions permits shaping of the shield as a means of reducing weight.

THERMAL AND HYDRAULIC ANALYSIS

In order to evaluate the potential capability of a small, liquid-metal cooled reactor, a thermal and hydraulic analysis was performed. Due to the preliminary nature of this study, the analysis was based on steady-state performance with no consideration for power transients or other abnormal conditions which might adversely affect reactor operation. Temperature distributions, flow requirements, and the resulting pressure losses were evaluated over a range of reactor sizes and operating power levels. Because of the apparent advantages of triangular spaced coolant holes for small, liquid-metal cooled reactors (see appendix), other fuel element geometries were not considered for the preliminary study.

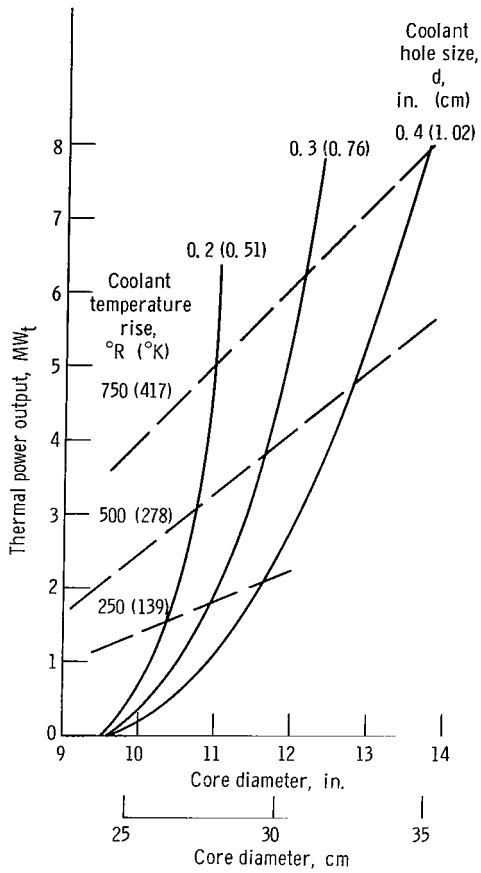

Figure 6. - Potential capability of lithium 7 cooled reactor. Effective multiplication factor, 1.10; core length-to-diameter ratio, 1.0; exit coolant temperature, 3000° R (1670° K); maximum fuel temperature, 3500° R (1945° K); fuel, uranium 233 dioxide.

Typical of the results obtained from these calculations are those shown in figure 6 where the potential power capability of the previously described $U^{233}O_2$ reactor system (fig. 1) is plotted for various operating conditions and coolant hole sizes. The maximum fuel temperature and the exit coolant temperature were maintained at 3500^{o} and 3000^{o} R (1945^{o} and 1670^{o} K), respectively. Coolant flow rates, inlet coolant temperatures, and the coolant temperature rise across the reactor were allowed to vary arbitrarily to study their effect on the reactor power

From figure 1, the smallest reactor possible with the $U^{233}O_2$ system was approximately 9.5 inches (24.1 cm) in diameter. However, since the allowable coolant fraction for this core is zero (fig. 1), it is obviously impossible to extract any useful power from this particular reactor. As the size and corresponding coolant fraction of the reactor was increased, the power removal capability increased rapidly. With 0.3-inch (0.75-cm) diameter coolant holes, for example, it would be possible to obtain approximately

2.5 MW_t from an 11.25-inch (28.6-cm) diameter core with approximately a 340° R (190° K) coolant temperature rise ΔT. To achieve this particular power output, however, several parameters were allowed to vary to values which may be difficult to obtain. Typical parameters required to obtain 2.5 MW_t from an 11.25 inch (28.6 cm) lithium-cooled reactor operating at an average exit coolant temperature of 3000° R (1670° K) are presented in table VIII.

TABLE VIII. - TYPICAL PARAMETERS FOR A LITHIUM COOLED REACTOR

Core power, MW_t	2.5
Average exit coolant temperature, °R; °K	3000; 1670
[a]Maximum fuel temperature, °R; °K	3500; 1945
Core diameter, in.; cm	11.25; 28.6
Core length-to-diameter ratio	1.0
Coolant hole diameter, in.; cm	0.3; 0.75
Hole spacing, in.; cm	2.7; 1.8
Coolant fraction	0.16
Coolant flow rate, lb/sec; kg/sec	7.0; 3.2
Coolant velocity, ft/sec; m/sec	2.4; 0.73
Reynolds number	1.9×10^4
Average heat-transfer coefficient, Btu/(hr)(ft^2)(°R); W/(cm^2)(°K)	7.3×10^3; 4.1
[a]Coolant ΔT, °R; °K	340; 190
Coolant inlet temperature, °R; °K	2660; 1480
Average heat flux, Btu/(hr)(ft^2); W/cm^2	0.53×10^6; 167
[a]Maximum heat flux, Btu/(hr)(ft^2); W/cm^2	0.90×10^6; 284
Pressure drop across reactor, psi; N/cm^2	<0.1; <0.07
[a]Maximum fuel burnup in 20 000 hr, atom percent	4.5

[a]Parameters that may limit the power capability of the reactor.

The parameters and their effect on reactor performance will be discussed in subsequent sections.

Note that with the relatively low flow rate required for the 2.5 MW_t, 340° R (190° K) ΔT design, the pressure losses across the reactor are less than 0.1 psi (<0.07 N/cm^2). The pressure loss shown includes the entrance and exit (contraction and expansion) losses and the frictional loss through the reactor core. No allowance has been made for orificing which may be required for flow stability, and the pressure losses in the pressure vessel, piping, heat exchanger, etc., have not been included. For increased flow rates, smaller coolant temperature rises or higher reactor power output, the pressure loss would, of course, increase. However, the flow rate can be increased considerably above the 7.0-pound-per-second (3.2 kg/sec) value without experiencing excessive pressure losses through the reactor. For example, if the flow rate were doubled, the pressure drop across the reactor would still be less than 0.5 psi (<0.35 N/cm^2). It can be concluded that the pressure loss through the core of a lithium-cooled reactor will be a relatively insignificant consideration in the selection of other operating parameters.

EFFECT OF VARIOUS PARAMETERS ON REACTOR SIZE REQUIREMENTS AND POWER REMOVAL CAPABILITY

In contrast to the pressure losses across the reactor, several of the operating conditions listed in table VIII do present some question with regard to feasibility. The sensitivity of reactor performance to each of these parameters was therefore explored in order to determine how fruitful the establishment of actual limiting values for these variables would be. These parameters are

(1) Allowable heat flux

(2) Allowable fuel temperature

(3) Allowable fuel burnup

(4) Allowable coolant temperature rise

The sensitivity (or lack of sensitivity) of the reactor to each of these parameters would then be used to determine the proper direction for future investigations.

To investigate each of the parameters listed, a study was performed using a 2.5-MW_t reactor with a core length-to-diameter ratio of 1.0. The results are discussed in the following sections.

Allowable Heat Flux

Since the maximum heat flux is a direct measure of the power being extracted from a given reactor configuration, it is obvious that, the greater the allowable heat flux, the greater the power capability of the reactor. As the heat flux and reactor power are increased to higher and higher values, temperatures within the reactor also increase and would eventually reach some allowable temperature limit that may have been imposed. However, before the temperature limit has been reached, it is possible that another limitation on heat flux may be reached. This limitation is the so-called "critical heat flux" which is associated with the inception of film boiling and which usually results in a sudden, large increase in the fuel element temperature.

As noted in the section BASIC ASSUMPTIONS, one advantage of using lithium as the liquid-metal coolant was to allow reactor operation at pressures of less than 50 psia (34.5 N/cm^2 abs) in order to minimize pressure stresses in structural components. The saturation temperature of lithium at this pressure is about 3250° R (1805° K) so that during nominal, steady-state operation, the maximum fuel element surface temperature would be 100° R (55° K) or more below the boiling point. However, it is possible that the combined uncertainties of predicting the radial and axial flux distributions, calculating heat-transfer coefficients, and tolerance deviations in manufacturing could result in local

TABLE IX. - MAXIMUM-TO-AVERAGE POWER FACTORS USED IN DETERMINATION OF EFFECT OF ALLOWABLE HEAT FLUX ON REACTOR SIZE

Factor	Value
Radial power distribution	1.10
Axial power distribution	1.20
Control swing	1.12
Hot channel allowance	1.15
Product	1.7

surface temperatures which approach or even exceed the saturation temperature (particularly, if transient conditions are considered). Under such conditions, it would be possible for local film boiling to occur if the heat flux at that point were greater than the critical value. At present there is no experimental data on the critical heat flux of lithium; however, available empirical equations (ref. 20) for predicting the critical heat flux of liquid metals indicate that lithium should be capable of sustaining fluxes in excess of 2×10^6 Btu per hour per square foot (630 W/cm^2). Experimental results for other liquid metals (i.e., sodium, potassium, rubidium, and cesium) show that heat fluxes of about 1×10^6 Btu per hour per square foot (315 W/cm^2) can be obtained (ref. 20). Therefore, to extend the available technology on critical heat flux of liquid metals to a high performance, lithium-cooled reactor, considerable experimentation would be required. To assess the potential gains which might result from such an experimental program, a series of calculations were performed on the 2.5-MW_t reactor covering a range of maximum allowable heat fluxes from 0.75×10^6 to 3.0×10^6 Btu per hour per square foot (236 to 946 W/cm^2). A maximum-to-average power factor of 1.7 was used on these calculations based on the assumed values shown in table IX.

Figure 7 shows the results of the calculations made for coolant hole sizes of 0.125- and 0.25-inch (0.32- and 0.64-cm) diameter, respectively. Superimposed on the results is the $U^{233}O_2$ criticality curve (i.e., $k_{eff} = 1.10$) from figure 1. The effect of increasing the allowable heat flux at a constant coolant fraction and for a given coolant hole size is quite pronounced. For example, for a coolant fraction of 0.10, the required size for a 2.5-MW_t reactor using 0.125-inch (0.32-cm) coolant hole (fig. 7(a)) decreases from 10.5 inches (26.6 cm) at an allowable flux of 0.75×10^6 Btu per hour per square foot (236 W/cm^2), to 6.5 inches (16.5 cm) at 3×10^6 Btu per hour per square foot (946 W/cm^2). The corresponding change for the 0.25-inch (0.64-cm) diameter coolant holes (fig. 7(b)) is from 13 to 8 inches (33 to 20.3 cm).

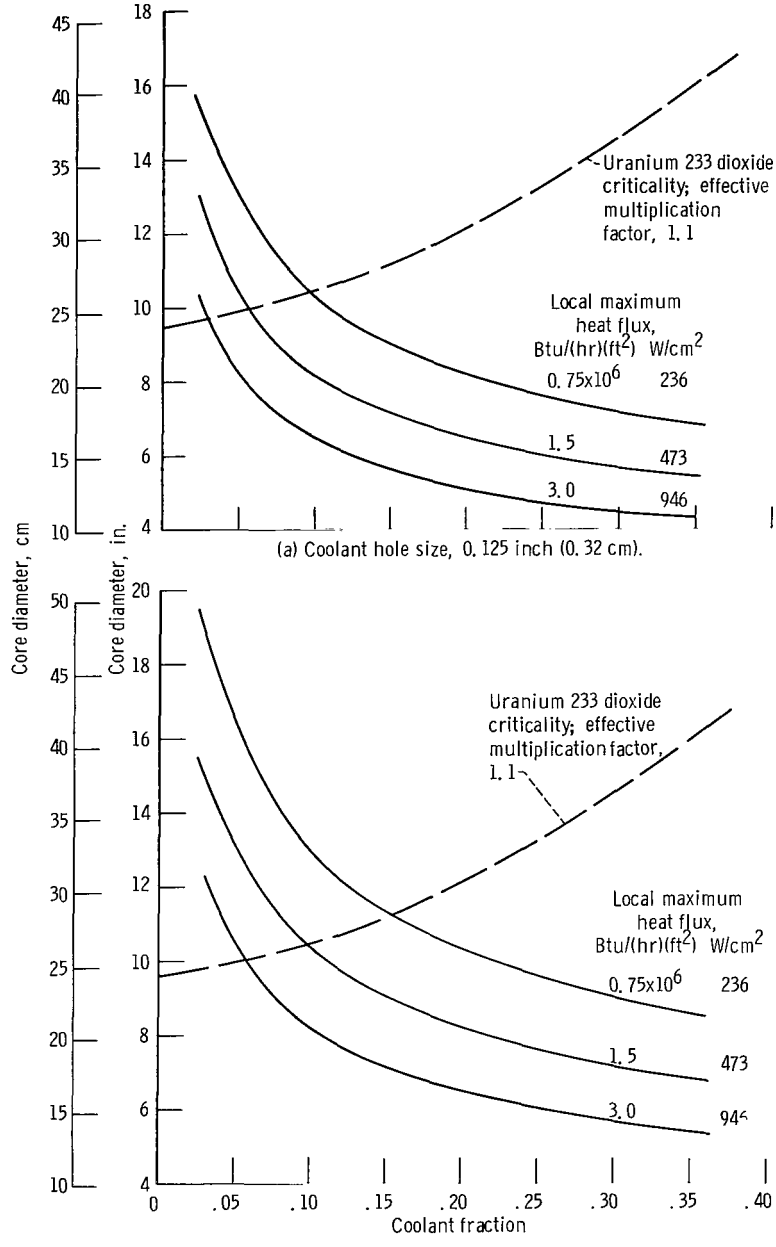

(a) Coolant hole size, 0.125 inch (0.32 cm).

(b) Coolant hole size, 0.25 inch (0.64 cm).

Figure 7. - Effect of allowable heat flux on required core size. Core length-to-diameter ratio, 1.0; core power, 2.5 megawatts thermal; local power factor, 1.7.

If, however, instead of comparing the results at a constant coolant fraction, the effect of increasing the allowable heat flux is considered in view of the nuclear criticality requirements for a given fuel composition, the results are not quite so significant. The variation in the required reactor size for the same range of heat fluxes is only 9.75 to 10.5 inches (24.8 to 26.7 cm) for the 0.125-inch (0.32-cm) diameter coolant holes and 10 to 11.25 inches (25.4 to 28.6 cm) for the 0.25-inch (0.64-cm) holes.

It can be concluded that, although maximum allowable heat flux does influence the size requirements for a given reactor configuration (i.e., a given coolant fraction and coolant hole size), the effect is minimized by a slight adjustment of the coolant fraction. Since nuclear criticality must also be maintained, the adjustment in coolant fraction can easily be made with a relatively small change in core size. For the range of reactor conditions considered in this study, therefore, it does not appear that an extensive experimental heat-transfer program would reduce the reactor size requirements significantly. As heat fluxes are increased beyond 0.75×10^6 Btu per hour per square foot (236 W/cm^2), the margin from the critical heat flux decreased with no appreciable gain in performance.

Allowable Fuel Temperature

Another variable which could seriously alter the size requirements of a high-temperature reactor is the maximum allowable fuel temperature. Obviously, the higher the allowable fuel temperature, the greater the power removal capability of a given reactor configuration operating at a specified coolant temperature.

From preliminary, experimental, out of pile data on the thermal cycling of tungsten-UO_2 fuels (ref. 6), it appears that operation of this fuel material with temperature gradients of 500° R (278° K) is feasible. Maximum fuel temperatures with a 3000° R (1670° K) coolant temperature would therefore be limited to approximately 3500° R (1945° K) based on thermal stress considerations. However, from preliminary irradiation data on various UO_2 fuels, indications are that fission product retention is strongly dependent on the fuel temperature. It would appear that lowering the maximum allowable fuel temperature to less than 3500° R (1945° K) could increase the fission gas retention and reduce thermal stresses in the fuel.

To determine how a reduction in allowable fuel temperature might affect the size and performance of the fast-spectrum, liquid-metal cooled reactors, calculations were first performed assuming an allowable maximum fuel temperature of 3500° R (1945° K). A second set of calculations were then made in which the allowable fuel temperature was reduced to 3375° R (1875° K), a 25 percent reduction in the difference between maximum fuel temperature and the 3000° R (1670° K) coolant temperature. Figure 8 shows the

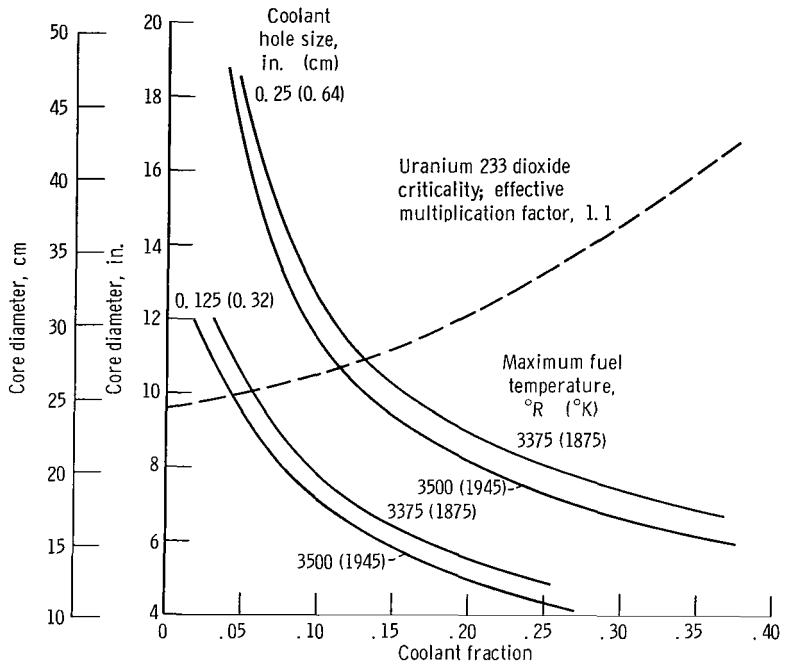

Figure 8. - Effect of allowable maximum fuel temperature on required core size. Core length-to-diameter ratio, 1.0; reactor power, 2.5 megawatts thermal; coolant temperature rise, 500° R (678° K); coolant exit temperature, 3000° R (1670° K).

results of this study for coolant hole sizes of 0.125 and 0.25 inch (0.32 and 0.64 cm) in diameter.

As in the case of the heat flux, the difference in required reactor size with allowable fuel temperature is very small if the coolant fraction is allowed to vary along the $U^{233}O_2$ criticality curve.

Table X summarizes the reactor size requirements for the various heat-transfer limits considered in figure 8. The maximum variation in required reactor size for all cases shown is only 1.5 inches (3.8 cm). Expressed in terms of the weight of the shielding-plus-reactor (fig. 5), the maximum variation is 3500 pounds (1585 kg), or less than 8 percent of the gross weight. For the two coolant holes sizes considered, the maximum heat flux limit of 0.75×10^6 Btu per hour per square foot (236 W/cm^2) is more restrictive (i.e., it determines the required reactor size) than either the 3500° or 3375° R (1945° or 1875° K) maximum fuel temperature limit.

Under the conditions covered in this study, therefore, it would appear that the effect of the various heat-transfer limits (i.e., heat flux or fuel temperature) on required reactor size and weight is of secondary importance. This conclusion could also be extended to the difference between coolant hole sizes since, for a given heat-transfer limitation, the weight of a reactor using 0.25-inch (0.64-cm) diameter coolant holes is less than 4 percent greater than for 0.125-inch (0.32-cm) diameter coolant holes. As the hole size

TABLE X. - EFFECT OF VARIOUS HEAT-TRANSFER LIMITS ON REQUIRED REACTOR SIZE FOR URANIUM 233 DIOXIDE CORE

[Length-to-diameter ratio, 1.0.]

Limiting condition		Coolant hole size		Required reactor size		Shield-plus-reactor weight[a]	
Maximum heat flux							
Btu/(hr)(ft^2)	W/cm^2	in.	cm	in.	cm	lb	kg
0.75×10^6	236	0.125	0.32	10.5	26.7	47 200	21 410
1.5	473	.125	.32	10.0	25.4	46 080	20 900
3.0	946	.125	.32	9.75	24.8	45 500	20 640
.75	236	.250	.64	11.25	28.6	49 000	22 225
1.5	473	.250	.64	10.4	26.4	47 000	21 320
3.0	946	.250	.64	10.0	25.4	46 080	20 900
Maximum fuel temperature							
^oR	^oK						
3500	1945	0.125	0.32	9.9	25.1	45 800	20 775
3375	1875	.125	.32	10.1	25.7	46 500	21 090
3500	1945	.250	.64	10.7	27.2	47 600	21 590
3375	1875	.250	.64	10.9	27.7	47 800	21 680
Maximum variation				1.5	3.8	3 500	1 585

[a]From fig. 5.

is increased, however, the required shielding-plus-reactor weight changes more rapidly. Figure 9 shows the effect of increasing the coolant hole size between 0.125 and 0.5 inch (0.32 and 1.27 cm) using the heat flux limitation of 0.75×10^6 Btu per hour per square foot (236 W/cm^2) and a maximum fuel temperature of 3375^o R (1875^o K). The heat-transfer limitation, which controls the required core diameter along the $U^{233}O_2$ criticality line, changes from a heat flux limit to a temperature limit as the size of the coolant hole increases. Required core diameters over the range of coolant holes sizes vary from 10.5 to 13 inches (26.7 to 33 cm). This represents a shielding-plus-reactor weight range (fig. 5) of 47 200 to 55 000 pounds (21 410 to 24 950 kg) or approximately a 16.5 percent variation in weight. While this is a reasonable incentive for trying to use the smaller holes, manufacturing and inspection procedures should also be considered in selecting the appropriate coolant hole size. Note that the 0.5-inch (1.27-cm) diameter coolant holes require a coolant fraction of nearly 25 percent; this is almost to a value where the use of solid fuel rods would become competitive with coolant holes from heat-transfer consideration (Appendix). Again the choice between using large diameter coolant holes or solid rod fuel elements should be influenced by manufacturing and inspection techniques.

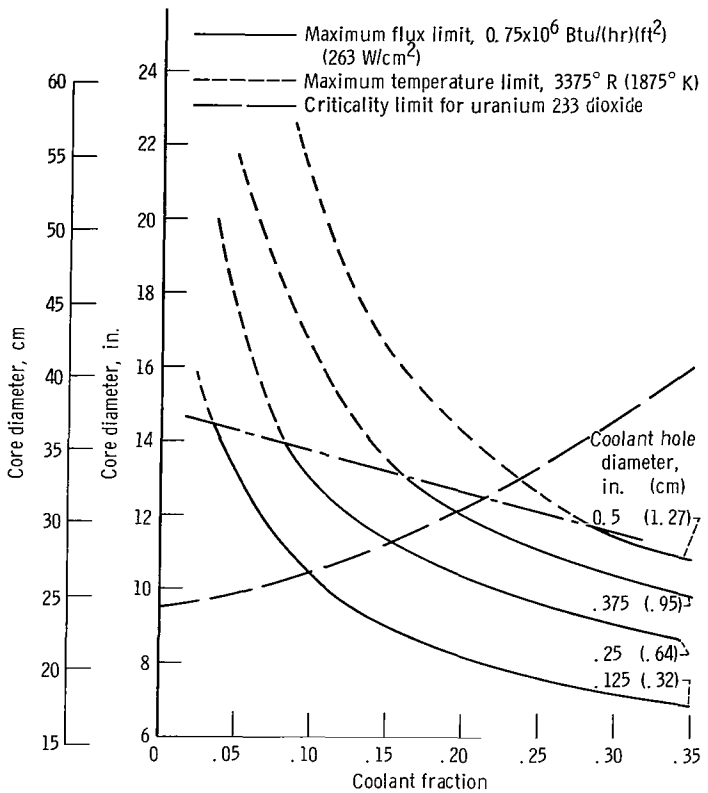

Figure 9. - Effect of heat transfer limits and coolant hole size on required core size. Core length-to-diameter ratio, 1; reactor power, 2.5 megawatts thermal; coolant temperature rise, 500° R (278° K); coolant exit temperature, 3000° R (1670° K).

Allowable Fuel Burnup

For small, high-power, long-life reactors, such as will be required for many space applications, a very important parameter in determining the capability of a given reactor configuration is allowable fuel burnup. If the 2.5-MW_t reactor were operated, for example, for 20 000 hours, the total number of uranium atoms which would be fissioned is about 5.6×10^{24} or nearly 5 pounds (2.3 kg) of uranium fuel. Depending on the reactor size, the type of fuel material, and fuel composition, the percentage of total uranium atoms which this represents can easily be established.

Using a radial and axial power factor of 1.1 and 1.2, respectively, the required reactor size necessary to produce various maximum fuel burnups was determined. Figure 10 shows the results of these calculations for $U^{233}O_2$ and $U^{233}N$ fuels with a 45-percent fuel, 45-percent tungsten, and 10-percent void composition. Curves for 2.0, 3.5, and 5.0 atom percent burnup are plotted to the point where they intersect the nuclear criticality (k_{eff} = 1.1) line.

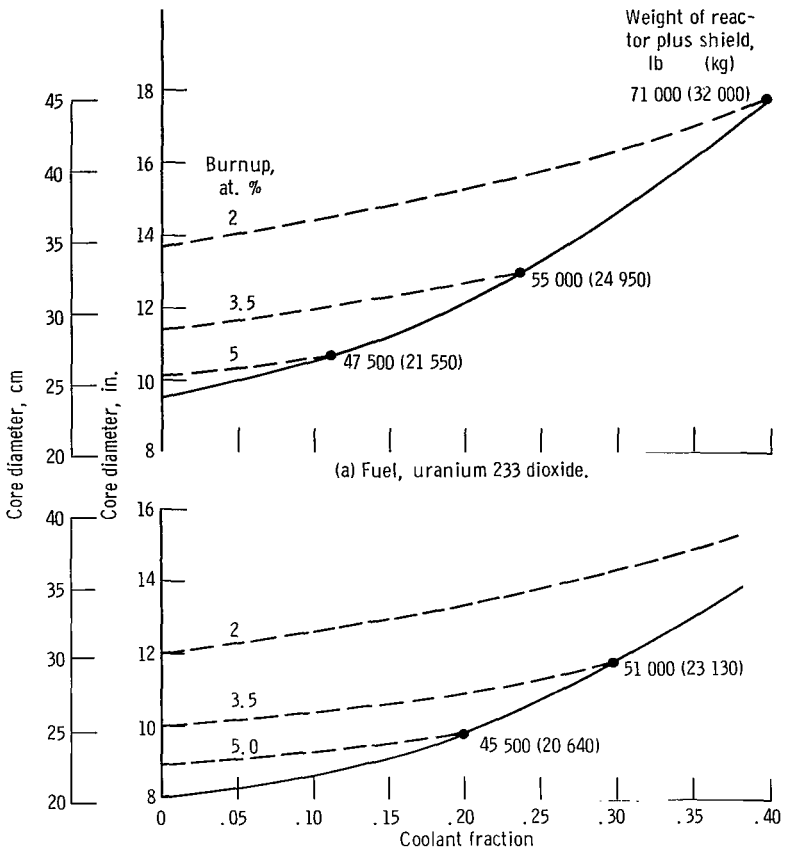

Figure 10. - Effect of allowable fuel burnup on required core size and weight of reactor plus shield. Effective multiplication factor, 1.10; core length-to-diameter ratio, 1.0; reactor power, 2.5 megawatts thermal; operating life, 20 000 hours. Fuel-matrix composition; fuel, 45 volume percent; tungsten, 45 volume percent; void, 10 volume percent.

As would be expected, the higher uranium density of the $U^{233}N$ fuel results in a smaller burnup fraction (approx. 33 percent less) than $U^{233}O_2$ fuel for the same size reactor. The effect of changing the allowable fuel burnup limit for either type fuel appreciably affects the size and weight of the reactors. For example, increasing the allowable fuel burnup from 2 atom percent to 5 atom percent for the $U^{233}O_2$ cores decreases the reactor-plus-shield weight from 71 000 to 47 000 pounds (32 200 to 21 300 kg).

This change is a much greater variation than occurred for either the heat flux or fuel temperature limits and emphasizes the importance of fuel burnup. Unfortunately, this is one area in which the allowable limits are not well defined and where an experimental program is definitely required. Although UO_2 fuels have operated in commercial power reactors with burnup as high as 3 to 5 atom percent without failing (ref. 21), swelling of the fuel appears to start at much lower values. If complete containment of

the fission products is attempted, the pressure increase due to accumulation of gaseous fission products may cause severe stress problems in the clad and matrix at these high temperatures. Allowable fuel burnups in this case may be as low as 2 atom percent. The use of vented fuel elements to relieve the gas pressure may increase the allowable fuel burnup significantly. However, behavior of these particular fuel materials under conditions of high temperature and long irradiation exposures must be established in order to define the allowable limit for both the vented and unvented systems.

Figure 10 also shows that, for the fuel compositions considered, there is little to gain from increasing the fuel burnup much beyond 5 atom percent since nuclear criticality becomes the limiting condition for the smaller reactors. Of course, if the operating life or reactor power level were changed, this conclusion also changes. For example, the 5 atom percent burnup curves (fig. 10) for a 20 000 hour, 2.5 MW_t reactor become 10 atom percent burnup curves if either the power or operating life of the reactor were doubled.

Since the maximum-to-average power factor used in these calculations was relatively small (i.e., $F_{max}/F_{avg} = 1.1 \times 1.2 = 1.32$), there is not much to be gained in this area, particularly since the reactivity requirements (and reactor size) will tend to increase with additional power flattening.

Allowable Coolant Temperature Rise Across the Reactor

For a given reactor power and exit coolant temperature, the coolant flow rate and coolant temperature rise across the reactor are inversely related: the higher the coolant flow rate, the smaller the coolant ΔT. Since many of the limits imposed on reactor performance are directly affected by changes in temperature and flow rates, the temperature rise across the reactor cannot be arbitrarily chosen but must be optimized for a given set of conditions and design objectives. Of course, the coolant flow rate and ΔT finally selected for the reactor must also be compatible with the requirements of the secondary system since they will affect the efficiency and performance of the electrical conversion cycle.

There are several factors (other than the reactor performance and secondary system requirements) which could influence the overall performance of a liquid-metal cooled, space-power reactor, and which must be considered in the final selection of the coolant temperature rise through the reactor. One of these is the problem of excessive material corrosion in the presence of temperature gradients in liquid-metal environments. While there appear to be several basic mechanisms of corrosion which can occur in liquid-metal systems (ref. 22), one corrosion process of particular interest is one in which structural material is dissolved into the liquid-metal in a high temperature zone and deposited in a

cooler zone. For a large difference between the reactor inlet and exit coolant temperatures, this "mass-transfer" corrosion process (ref. 22) could seriously affect fuel element integrity. Experimental corrosion programs are presently being conducted at Lewis to determine the magnitude of this problem in lithium-cooled systems.

Other factors directly affected by changes in the coolant temperature rise and flow rate through the reactor loop are coolant velocities, pressure losses in the sytem, pumping power requirements, operating temperature of the pump, thermal stresses caused by coolant temperature differences, and the required size and weight of systems components (e.g., piping and heat exchanger). The effect on the weight of these auxiliary components must, of course, be compared with the effect on the weight of the reactor and shield, since a net weight savings could be realized even though the heat exchanger weight, for example, might increase.

Coolant flow rate and coolant ΔT, therefore, directly or indirectly influence many parameters and each of these must be considered in selecting the proper coolant temperature rise and flow rate for the reactor. For the reactors considered in this study, the effect of the coolant ΔT depends on the choice of coolant hole size selected. Figure 9 shows that near the nuclear criticality line, heat flux is limiting for the smaller coolant hole sizes while fuel temperature becomes limiting for the larger holes. When heat flux is the limiting condition, there is obviously nothing to be gained in reactor performance by changing coolant temperatures or flow rates. However, when maximum fuel temperature (or any structural temperature) limits the operation of the reactor, it is possible to improve performance (or reduce reactor size) by changing the coolant temperature rise or lowering the exit coolant temperature. Since a reduction in the exit coolant temperature adversely affects the overall thermodynamic efficiency of most systems and requires larger heat rejection equipment, the 3000° R (1670° K) exit coolant temperature was considered desirable, and only the effect of varying the coolant ΔT was considered in this preliminary analysis.

To illustrate the results of changing coolant ΔT, a range of achievable reactor sizes was defined from the results of the previous study of heat flux, fuel temperature, and fuel burnup limitations. It was assumed that coolant holes sizes of from 0.125- to 0.25-inch (0.32- to 0.64-cm) diameter were feasible and that fuel burnups in the range of from 2 to 5 atom percent could be attained either with or without venting the fuel. With these assumed limiting conditions, an envelope (fig. 11) which defines the potential reactor size range for a 2.5-MW_t system was constructed based on the results obtained for a coolant ΔT of 500° R (278° K). It can be seen that only a small portion of the envelope is limited by temperature considerations (i.e., from point 4 to point 5 on fig. 11). An estimate of the specific weight (i.e., weight per kW electric) of the reactor plus shield is also shown for four locations on the envelope. Variations in the specific weight are from 95 pounds per electrical kilowatt (kW_e) to 119 pounds per kW_e (43 to 54 kg/kW_e) for

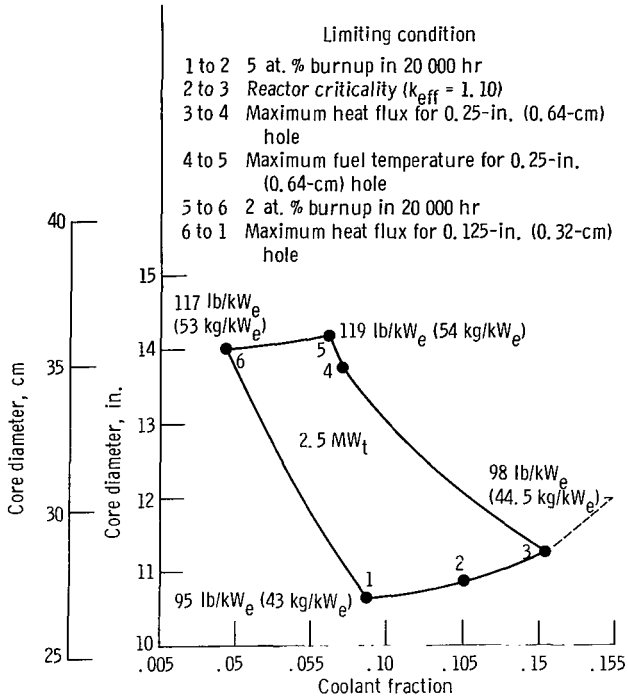

Figure 11. - Specific reactor-plus-shield weight envelope for fast-spectrum, lithium 7 cooled reactor for various restricting conditions. Core length-to-diameter ratio, 1.0; fuel, uranium 233 dioxide; assumed efficiency, 20 percent; electrical power, 500 kilowatts electric; coolant temperature, 3000° R (1670° K); coolant temperature rise, 500° R (278° K).

the conditions considered and assuming a cycle efficiency of 20 percent. The change in specific weight with allowable fuel burnup causes most of the difference.

Figure 12 shows the effect of changing the coolant ΔT. Only a very small change in the size of the limiting envelope results from reducing the coolant ΔT from 500° to 100° R (278° to 55.5° K). For a given coolant fraction (e.g., 8 percent), the required size of the reactor increases for a reduction in coolant ΔT. Since a reduction in coolant ΔT for a constant reactor power requires an increase in the coolant flow rate, the change in core size implies that lower coolant flow rates are better than higher coolant flow rates. While this may seem anomalous, the condition results from several related factors:

(1) Throughout the study, the exit coolant temperature was held constant. An increase in coolant ΔT (decrease in coolant flow rate) was accomplished by lowering the inlet temperature. The coolant temperature was, therefore, lower over most of the reactor length.

(2) The heat-transfer characteristics of liquid-metals under forced convection are excellent (even at low flows), and the temperature difference between coolant and surface is small relative to the temperature gradient through the fuel material (see the appendix).

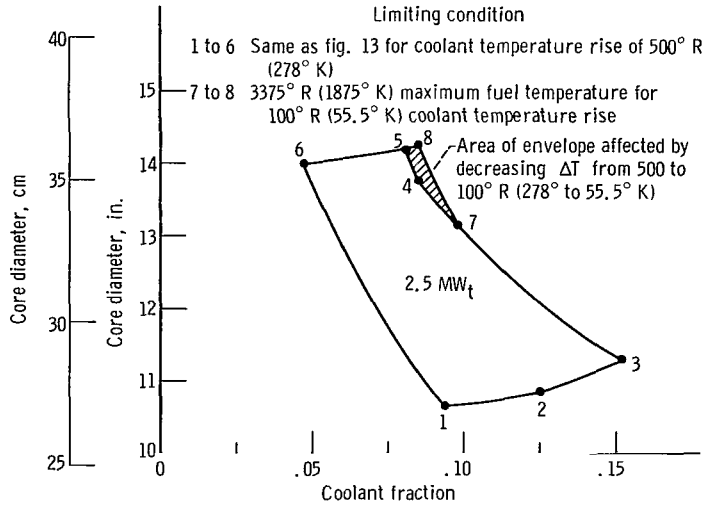

Figure 12. - Effect of changing coolant temperature rise of 2.5-megawatt thermal power reactor from 500° to 100° R (278° to 55.5° K). Core length-to-diameter ratio, 1.0; fuel, uranium 233 dioxide; coolant temperature, 3000° R (1670° K).

Any decrease in the heat-transfer rate associated with a reduction in coolant flow is, therefore, insignificant compared with the reduction in coolant temperature at the point of maximum temperature.

For small coolant hole sizes, the effect of coolant ΔT on reactor size and performance is negligible. The final coolant ΔT should, therefore, be selected based on all the factors that are influenced by coolant temperature and flow rate.

Effect of Reactor Power Level

All the preceeding comparisons were made on a 2.5-MW_t reactor. To determine how the power level might influence reactor size requirements, calculations were made on a 1.25- and a 5-MW_t reactor. The same coolant hole sizes, heat flux, fuel temperature, and fuel burnup limits were used to define a range of reactor sizes for these power levels. Figure 13 shows the results of this analysis and the corresponding 2.5-MW_t reactor analysis shown in figure 11. The envelope for all three power levels have essentially the same shape and are, in general, bounded by the same constraints. However, the lower boundaries of the three cases are different: for the 1.25-MW_t reactor the lower boundary is limited by nuclear criticality, for the 5-MW_t design by 5 atom percent fuel burnup, and for the 2.5-MW_t case by a combination of these two limits (fig. 11). Since the upper and lower boundary of the 1.25 MW_t reactor are quite close, the size of small power reactors are essentially fixed by nuclear consideration only. The limits on the larger reactors

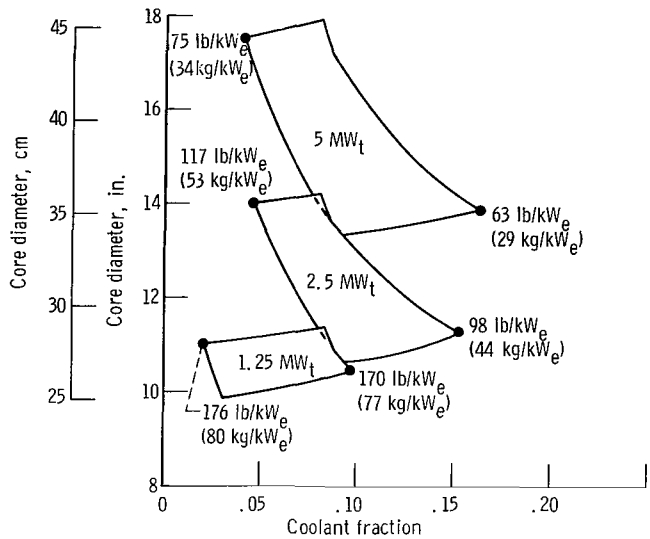

Figure 13. - Effect of reactor power level on specific reactor-plus-shield weight. Core length-to-diameter ratio, 1; fuel, uranium 233 dioxide; assumed efficiency, 20 percent; coolant temperature, 3000° R (1670° K); coolant temperature rise, 500° R (278° K).

allow for greater variation in required reactor sizes and, therefore, would benefit most from an experimental program which would establish the allowable fuel burnup limits.

While the size requirements of the reactors increase quite rapidly with power level, the specific weight of the reactor plus shield decreases significantly. Typical specific weights of the three reactor sizes are, respectively, 170, 110, and 70, (77, 50, and 32 kg/kW$_e$) for the 1.25-, 2.5-, and 5-MW$_t$ reactors. The specific weights were determined using an assumed 20 percent efficiency, the reactor-plus-shield weights from figure 5 and the 4500-pound (2040-kg) correction factor previously determined in the section SHIELD WEIGHT REQUIREMENTS.

CONCLUDING REMARKS

Based on the preliminary analysis of a fast-spectrum, liquid-metal (lithium) cooled, nuclear reactor for space-power applications, several conclusions and recommendations were made. These conclusions are based on the results obtained for a particular reactor system under a given set of assumptions, and do not necessarily apply to all fast-spectrum, liquid-metal cooled reactors.

1. The use of uranium^{233} (U^{233}), instead of uranium 235 (U^{235}), decreases the critical size of the reactors studied significantly. At a coolant fraction of 10 percent, for example, the required size of a reactor with a length-to-diameter ratio of 1.0, a 4-inch

(10.16-cm) tungsten reflector, and with 45 volume percent uranium dioxide in the fuel matrix is 10.5 and 17.4 inches (26.7 and 44.2 cm), respectively, for the $U^{233}O_2$ and $U^{235}O_2$ fuels.

2. The use of uranium nitride instead of uranium dioxide fuel also reduces the critical size of the reactors. Under the same conditions, the critical size of a uranium^{233} nitride reactor is 8.6 inches (21.8 cm) compared with the 10.5 inches (26.7 cm) required for uranium^{233} dioxide fuel.

3. Because of the higher uranium density in uranium nitride fuels, the fuel burnup is lower than in a comparable uranium dioxide fuel by approximately 33 percent for the same size reactor and a given set of operating conditions.

4. The fuel loading can be increased to reduce the minimum size of the fast-spectrum reactors. The use of higher fuel loadings might also be a method of reducing fuel burnup for a given size core.

5. Throughout the study it was assumed that adequate nuclear control could be obtained, and an allowance in the excess reactivity of 10 percent was included for control and power flattening. However, it is not presently known whether the Doppler coefficient of fast-spectrum, uranium^{233} reactors is positive or negative. Future experiments must be performed to determine whether these reactors are easily controlled or whether inherent control must be engineered into the design.

6. Shielding weights are strongly dependent on whether complete or partial shielding is required. Assuming an allowable radiation dose of 2 millirem per hour at a point 66 feet (20 m) in any direction from the center of the core, the weight of biological shielding plus reactor for a 10-inch (25.4-cm), 2.5-MW_t reactor was calculated to be 46 080 pounds (20 920 kg). About half of this weight represents the shielding necessary to suppress secondary gammas which are produced in the tungsten gamma-shielding material.

7. A factor of two change in either reactor power or allowable dose rate would change the shield-plus-reactor weight by only 6 to 10 percent.

8. Allowable fuel burnup affects the reactor size requirements considerably. Reactor-plus-shield weight for a 5 atom percent burnup limited reactor is about two-thirds that for a 2 atom percent burnup limit. Experimental data are required to establish maximum fuel burnup limits for vented and unvented systems.

9. For the temperature range considered in this study, limitations imposed by steady-state heat transfer (i.e., heat flux and fuel temperatures) do not change the required reactor size and weight significantly. The size of the reactors considered in this study varied by only 1.5 inches (3.8 cm) over a wide range of heat fluxes and fuel temperatures. It does not appear that an extensive liquid-metal heat-transfer program would be justified on the basis of potential improvement in reactor performance.

10. The effects of coolant flow rates, coolant temperatures, and coolant temperature

rise are of secondary importance in determining the size of the reactor studied. These parameters should, therefore, be selected based on the overall system requirements (e.g., pumping power, heat exchanger size, material limitations, and corrosion effects).

11. The effect of increasing reactor power level causes an increase in required reactor size, but the specific weight-to-power ratio decreases significantly. A 5 MW_t reactor has a specific weight of approximately 70 pounds per electrical kilowatt (32 kg/kW_e) whereas the corresponding value for a 1.25 MW_t reactor is 170 lb/kW_e (77 kg/kW_e).

Lewis Research Center,
National Aeronautics and Space Administration,
Cleveland, Ohio, August 25, 1967,
120-27-06-17-22.

APPENDIX - COMPARISON OF TRIANGULAR-SPACED COOLANT HOLES AND SOLID-ROD FUEL ELEMENTS FOR USE IN SMALL, FAST-SPECTRUM, LIQUID-METAL COOLED NUCLEAR REACTOR

In determining the power removal capability of the liquid-metal cooled reactor systems analyzed in this study, the fuel element geometry was assumed to be triangular-spaced coolant holes in a solid matrix. One of the reasons for this selection was that holes are capable of providing the low coolant fractions which are desirable for small, fast-spectrum reactors. Solid rods, for example, have a definite limitation (9.3 percent) on the minimum coolant fraction which can be achieved (fig. 14), and the slope of coolant fraction as a function of spacing-to-diameter ratio is also quite steep in the low coolant fraction region. Conversely, holes in a solid matrix essentially have no minimum coolant fraction (fig. 14), and the sensitivity to changes in spacing is quite small for coolant fraction of less than 25 percent.

To compare the relative sensitivity of holes and rods, consider an initial coolant fraction of 10 percent. For the case of holes in a solid matrix, a changing in the spacing-to-diameter ratio s/d of 16.7 percent (from 3.0 to 2.5) increases the coolant fraction by only 4.5 percent (from 0.10 to 0.145). A similar change in the spacing-to-diameter

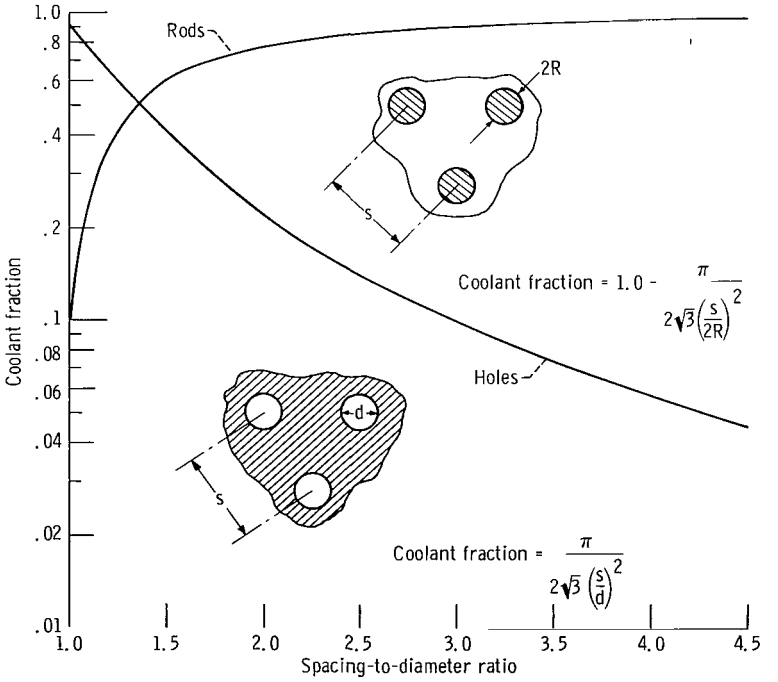

Figure 14. - Effect of spacing-to-diameter ratio on coolant fraction of solid rods and coolant holes with triangular spacing.

ratio (s/2R) of rods (i.e., 16.7 percent) increases the coolant fraction from 0.10 to 0.335. The increased sensitivity of the rods to dimensional variations would require much closer tolerance control in assembly and manufacturing and could conceivably increase the value of the hot channel factors normally applied to the thermal analysis of reactors. It is possible, however, that maintaining close tolerances on rods might be easier than the problems associated with inspecting relatively long, small diameter holes in a matrix type fuel element.

A second consideration in the use of holes rather than rods in the analysis of the small, fast-spectrum reactors, is the potential problem of nonuniform circumferential temperature distributions associated with the flow of liquid metal in closely spaced rods. Dwyer (ref. 23) notes that for closely spaced rods cooled by liquid metals, variations of the local heat-transfer coefficient about the circumference of the rod are quite dependent on the spacing-to-diameter ratio as shown in table XI.

Magee and Tromel (ref. 24) have analyzed the SNAP 8 fuel element and determined that the circumferential heat-transfer coefficient for a 0.56-inch (1.42-cm) rod varies by approximately a factor of 2 to 4 with a spacing-to-diameter ratio of 1.02 to 1.04 (coolant fraction of 0.13 to 0.16). The apparent disagreement between these values and those of Dwyer (ref. 23) are attributed (ref. 24) to the difference between the boundary conditions assumed in the two analyses. Both studies, however, agree that, above a coolant fraction of 50 percent ($s/2R > 1.35$), no circumferential variation should occur.

In addition to the local, circumferential variation, the average heat-transfer coefficient also decreases with the spacing-to-diameter ratio of rods. When the rods are touching, for example, the average heat-transfer coefficient can be determined (ref. 23) from the relation

$$Nu = 0.120\ Pe^{0.4} \tag{A1}$$

TABLE XI. - VARIATION IN CIRCUMFERENTIAL HEAT-TRANSFER COEFFICIENT WITH SPACING-TO-DIAMETER RATIO OF CLOSELY SPACED RODS

Spacing-to-diameter ratio, s/2R	Coolant fraction	Circumferential variation of heat-transfer coefficient (a)
1.375	0.52	1.2
1.2	.37	1.7
1.1	.25	~100

[a] From ref. 23.

where

Nu Nusselt number, hD_e/K_1

Pe Péclet number

h film coefficient

D_e equivalent hydraulic diameter

K_1 thermal conductivity of the liquid metal

If this relation (eq. (A1)) is compared with the Lubarsky-Kaufman correlation (ref. 25) for the flow of liquid metal in tubes,

$$Nu = 0.625\ Pe^{0.4} \tag{A2}$$

it can be seen that the average heat-transfer coefficient for tightly packed rods is approximately five times smaller than for the case of flow in circular tubes at the same flow rate and equivalent hydraulic diameter. This agrees quite well with the SNAP 8 analysis (ref. 24) where the calculated average heat-transfer coefficient for rods with a spacing-to-diameter ratio of 1.018 was about one-fourth that of flow in circular tubes of equivalent hydraulic diameter. Experimental studies by Subbotin, et al. (ref. 26), at spacing-to-diameter ratios of 1.2 and 1.1, qualitatively substantiate the decrease in the average heat-transfer coefficient with decreasing spacing-to-diameter ratios. However, there appears to be some question about the accuracy of Subbotin's results at low Péclet numbers (ref. 23 and 24).

While there are insufficient data to accurately predict the extent of the reduced liquid-metal heat-transfer coefficient for closely spaced rods, presently available experimental and analytical studies indicate that such a reduction does occur. The effect of this reduced heat-transfer coefficient is only important in the way in which it alters the temperature of the fuel and clad. If the heat flux is relatively low and the heat-transfer coefficient high, an average or circumferential factor of 4 or 5 may only represent a very small temperature variation. However, if the heat flux, for example, were as high as 1.5×10^6 Btu per hour per square foot (473 W/cm^2) and the heat-transfer coefficient were on the order of 10 000 Btu per hour per square foot per ^oR (5.7 $W/(cm^2)(^oK)$), the temperature difference between coolant and the fuel element surface would be 150^o R (83^o K). A reduction of 4 or 5 in the average or local heat-transfer coefficient under such conditions could be serious if the fuel elements were already operating near some temperature limit.

Because the operating temperature of the fuel is an important consideration for many

applications, another factor which must be considered in comparing rods and coolant holes is the temperature drop through the fuel materials. To simplify the comparison between rods and coolant holes, it is assumed that the fuel material and clad are bonded and can be treated as a homogeneous material. The equation governing one-dimensional steady-state heat conduction in a rod with internal heat generation (ref. 27) is given by

$$\left(T_{max} - T_s\right)_{r,z} = F_{r,z} Q \frac{R^2}{4K} \tag{A3}$$

where

T_{max} maximum internal temperature of fuel

T_s surface temperature

Q average volumetric heat generation rate

$F_{r,z}$ local peak-to-average power factor of core at axial z and radial r location being considered

K mean thermal conductivity of the fuel element

R radius of the rod

For the case of coolant holes of diameter d and with spacing s, the semiemperical equation of Sparrow (ref. 28) is used

$$\left(T_{max} - T_s\right)_{r,z} = F_{r,z} \frac{Q}{K}\left(\frac{s}{2}\right)^2 \left[\left(\frac{\sqrt{3}}{\pi}\right)\ln\left(\frac{s}{d}\right) + 0.25\left(\frac{d}{s}\right)^2 - 0.23466\right] \tag{A4}$$

Obviously, it would be difficult to compare the temperature differences resulting from these two equations directly, since the terms in the two relations are different. It is possible, however, to simplify the comparison of these expressions by the use of the equivalent hydraulic diameter D_e and the coolant fraction C_f of the core. For a given reactor size and operating power level, the determination of nearly every geometric hydraulic, heat-transfer, and nuclear parameter is in turn fixed by the choice of these two variables. Table XII lists several of the parameters used in the hydraulic and heat-transfer analysis. For the same equivalent hydraulic diameter and coolant fraction, the flow area, surface area, heat flux, heat generation rate, and frictional pressure drop are identical for both solid rods or coolant holes if the reactor volume V, power level q, and flowrate W are the same. This generalization does not include local nuclear or heat-transfer factors, such as the circumferential heat-transfer coefficient, which may be related to a specific fuel element geometry.

TABLE XII. - PARAMETERS USED IN HYDRAULIC AND HEAT TRANSFER COMPARISON OF SOLID RODS AND COOLANT HOLES EXPRESSED IN TERMS OF THE EQUIVALENT DIAMETER AND COOLANT FRACTION

	Rods	Holes
Characteristic dimensions	R, S, L	d, S, L
Cell size (triangular pitch)	$\frac{\sqrt{3}}{2}S^2$	$\frac{\sqrt{3}}{2}S^2$
Coolant fraction, C_f	$1 - \frac{\pi}{2\sqrt{3}\left(\frac{s}{2R}\right)^2}$	$\frac{\pi}{2\sqrt{3}\left(\frac{s}{d}\right)^2}$
Equivalent hydraulic diameter, D_e	$2R\left(\frac{C_f}{1 - C_f}\right)$	d
Ratio of heat transfer area-to-core volume, A_s/V	$\frac{4C_f}{D_e}$	$\frac{4C_f}{D_e}$
Flow area, A_f	$C_f \frac{V}{L}$	$C_f \frac{V}{L}$
Surface heat flux, q/A_s	$\frac{qD_e}{4C_fV}$	$\frac{qD_e}{4C_fV}$
Average volumetric heat generation rate, Q	$\frac{q}{(1 - C_f)V}$	$\frac{q}{(1 - C_f)V}$
Frictional pressure loss, ΔP	$\frac{fL^3W^2}{2\rho g D_e (C_f V)^2}$	$\frac{fL^3W^2}{2\rho g D_e (C_f V)^2}$
Dimensionless temperature difference, ΔT^*	$\frac{1}{16}\left(\frac{1 - C_f}{C_f^2}\right)$	$\frac{1}{16}\left[\frac{C_f - \ln C_f - 0.9489}{C_f(1 - C_f)}\right]$
Dimensionless thermal stress or strain, σ^*, ϵ^*	$\frac{1}{32}\left(\frac{1 - C_f}{C_f^2}\right)$	$\frac{1}{16}\left[\frac{2C_f - 0.5C_f^2 - \ln C_f - 1.5}{C_f(1 - C_f)^2}\right]$

The dimensionless temperature difference ΔT^* shown in table XII is defined by

$$\Delta T^* = \frac{K(T_{max} - T_s)}{F_{r,z} \left(\frac{q}{V}\right) D_e^2} \tag{A5}$$

All terms contained in this expression (except, of course, the maximum fuel temperature) are independant of fuel element geometry. The value of the dimensionless temperature difference for specific fuel element geometry is found by rewriting the heat conduction equations (eqs. (A3) and (A4)) in terms of the equivalent diameter and the coolant fraction of the core. For the case of solid rods, the dimensionless temperature difference is

$$\Delta T^* = \left[\frac{1 - C_f}{16\, C_f^2}\right] \tag{A6}$$

and, for coolant holes in a solid matrix,

$$\Delta T^* = \left[\frac{C_f - \ln C_f - 0.9489}{16\, C_f(1 - C_f)}\right] \tag{A7}$$

Figure 15 shows a comparison between the dimensionless temperature difference for rods (eq. (A6)) and coolant holes (eq. (A7)). Under the same conditions, coolant holes have a significantly lower temperature drop through the fuel than rods. For example, at a coolant fraction of 15 percent, the dimensionless temperature difference for holes is 0.54 while that of rods is 2.36, a factor of over four on the temperature rise through the fuel material.

Bussard and De Lauer (ref. 27) have extended this type of comparison to include thermal stresses in the fuel material. In terms of the dimensionless temperature difference (eq. (A5)), the dimensionless elastic thermal stress σ^* can be expressed as

$$\sigma^* = \frac{\sigma_{th}(1 - \nu)\Delta T^*}{E\alpha(T_{max} - T_s)} \tag{A8}$$

where

σ_{th} elastic thermal stress

ν Poisson's ratio

E Young's Modulus

α thermal coefficient of expansion

For both the rod and the coolant hole, the maximum stress occurs at the coolant surface where the axial and tangential stresses are equal, so that Hooke's law (ref. 29) can be used to rewrite the stress relation in terms of a dimensionless thermal strain ϵ^*

$$\epsilon^* = \frac{\epsilon_{th}\,\Delta T^*}{(T_{max} - T_s)} \tag{A9}$$

where ϵ_{th} elastic thermal strain.

For the case of holes on a triangular pitch, the approximate relation for the dimen-

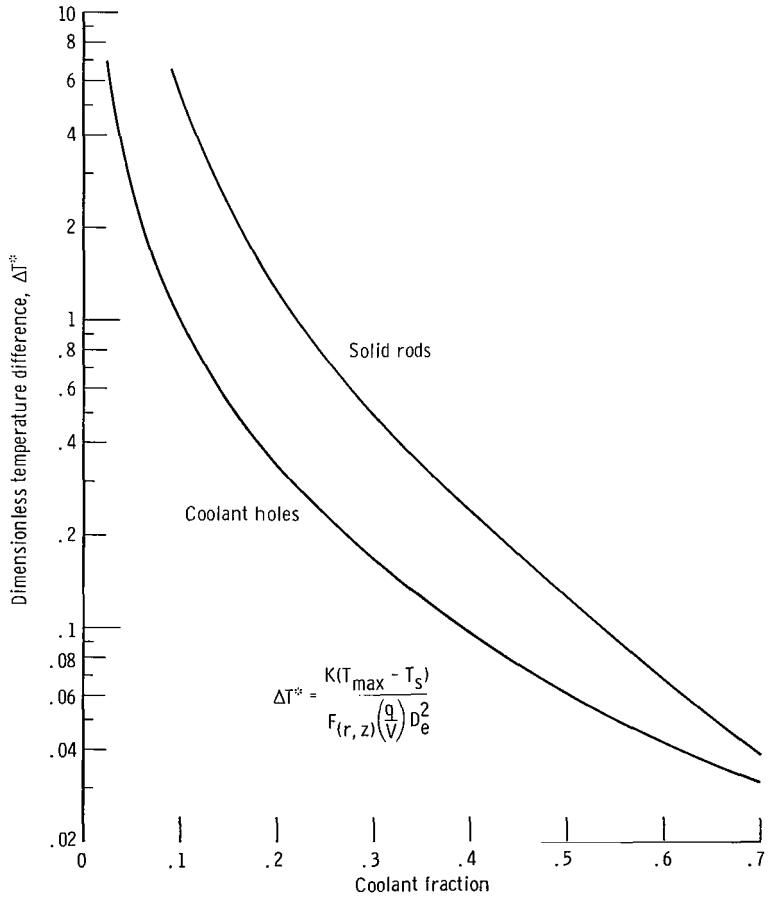

Figure 15. - Effect of coolant fraction on dimensionless temperature difference for solid rods and coolant holes.

sionless thermal stress or strain parameter (ref. 27) is

$$\sigma^* = \epsilon^* = \left[\frac{2C_f - 0.5\,C_f^2 - \ln C_f - 1.5}{16\,C_f(1 - C_f)^2}\right] \tag{A10}$$

A similar expression can be found for rods using the relations derived in reference 27. For solid rods, the dimensionless thermal stress or strain is one-half the value of the dimensionless temperature difference (eq. (A6)) or

$$\sigma^* = \epsilon^* = \left[\frac{1 - C_f}{32\,C_f^2}\right] \tag{A11}$$

Figure 16 is a plot of the dimensionless stress or strain parameter for rods and

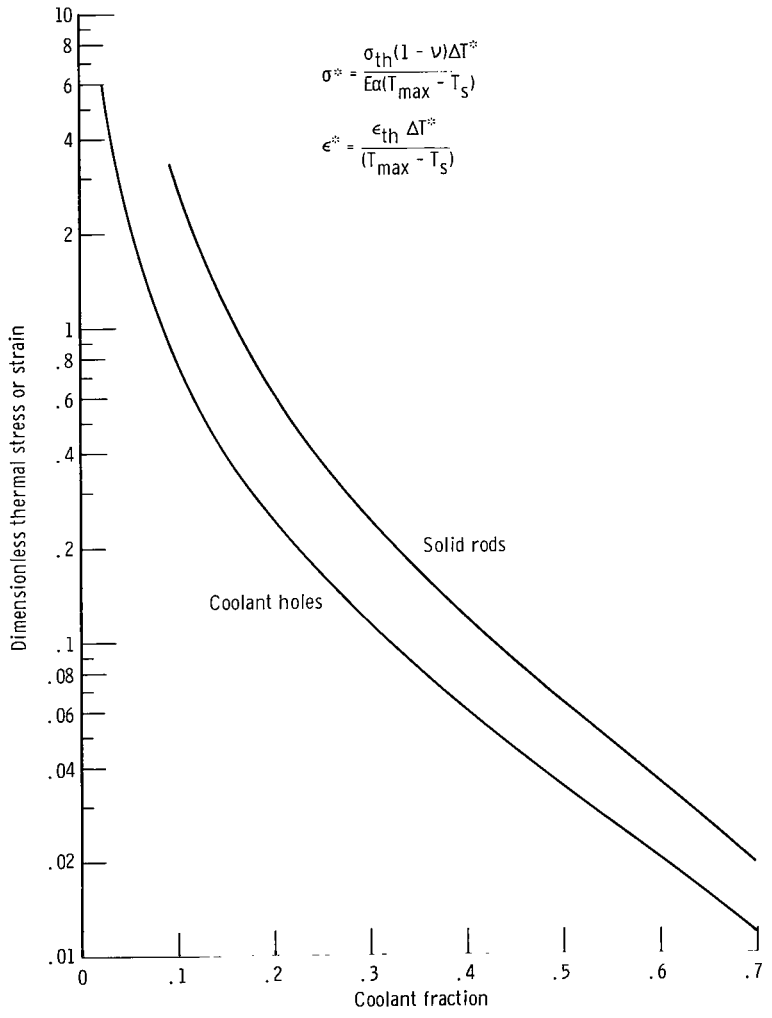

Figure 16. - Effect of coolant fraction on dimensionless thermal stress or strain of solid rods and coolant holes.

holes. As in the case of temperature difference (fig. 15), holes have a lower value than rods for the same conditions although the relative difference is not as great. Using the previous 15-percent coolant fraction example, the value of the thermal stress or strain parameter for holes is approximately 0.4, whereas that of the rods is 1.2 or a factor of three higher.

Therefore, it can be concluded that, for the same size reactor operating at the same power level and with the same flow rate and pressure loss, the temperatures and thermal stresses in a matrix type fuel element with triangular-pitch coolant holes will be less than in a comparable rod type fuel element. Since the dimensionless temperatures difference (eq. (A5)) and the dimensionless stress or strain parameter (eqs. (A8) and (A9)) varies as the square of the equivalent hydraulic diameter, it would be possible to reduce the temperatures and stresses in the rod to the same level as in the matrix type element by simply decreasing the equivalent hydraulic diameter. At a coolant fraction of 15 percent, for example, a decrease in the hydraulic diameter of a factor of two would offset the inherently higher temperature gradient in the rod element. Of course, a reduction in the equivalent hydraulic diameter would increase the frictional pressure loss ΔP_f across the core by a similar amount (table XII) but, as in the case of the low flow liquid-metal systems considered in this study, the frictional pressure loss may be low enough to permit such an increase. There are situations, however, where a factor of two increase in the pressure drop across the reactor could not be tolerated, and the use of coolant holes, rather than solid rods, would appear to be necessary.

The combined effect of (1) possible reduction in the average heat-transfer coefficient, (2) circumferential variations in the local heat-transfer coefficient, (3) higher temperatures in the fuel material, and (4) larger thermal stresses makes the use of closely packed rods unsuitable for high performance, cermet fueled nuclear reactors with small (<35 percent) coolant fractions. If fuel element manufacturing, inspection, and assembly procedures dictates the use of rod type fuel elements, rather than holes in a solid matrix, it would probably be necessary to increase the coolant fraction of the reactor to more than 35 percent ($s/2R > 1.2$) in order to minimize the effect of the reduced heat-transfer coefficient associated with closely spaced rods. Because the use of small coolant fractions (i.e., <35 percent) reduces the size of the fast-spectrum reactors considerably (figs. 1 to 3), the thermal analysis for this study was performed for holes in a solid matrix (triangular spacing). The fluid temperature distribution along a given coolant passage was determined integrating the local power input into the channel.

$$T_{b_{(r,z)}} = T_{in} + \frac{\pi d\, \varphi_{avg} \int_0^z F(r,z)dz}{W_r C_p} \qquad \text{(A12)}$$

where

T_b	bulk coolant temperature
T_{in}	inlet coolant temperature
d	coolant hole diameter
φ_{avg}	average heat flux
F	local peak-to-average power factor of core
W	channel coolant flow rate
C_p	specific heat of coolant
z	axial location
r	radial location

Surface temperatures were determined from the relation

$$(T_s - T_b)_{r,z} = F_{r,z} \frac{\varphi_{avg}}{h} \tag{A13}$$

where the heat-transfer coefficient h was calculated using the Lubarsky-Kaufman correlation (eq. (A2)). Maximum fuel temperatures were calculated using the semiempirical relation of Sparrow (eq. (A4)) and the thermal conductivity of the various fuel-matrix compositions was determined from the equations presented in reference 30. A typical temperature distribution obtained using the procedure is shown in figure 17.

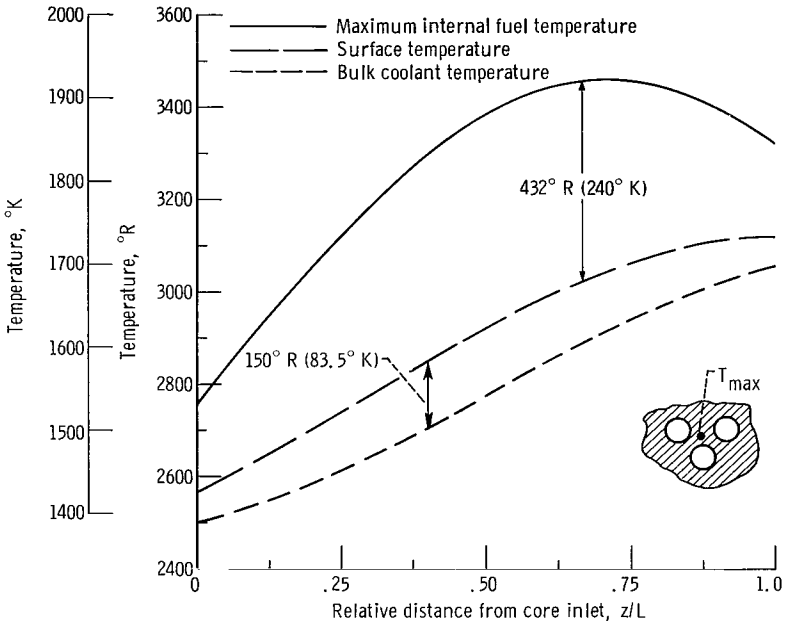

Figure 17. - Typical temperature distributions in lithium cooled reactor. Power, 2.5 megawatts thermal; average coolant temperature rise, 500° R (278° K); racial power factor, 1.10; coolant fraction, 0.10; maximum heat flux, 1.5×10^6 Btu per hour per square foot (473 W/cm^2); average exit temperature, 3000° R (1670° K); inlet coolant temperature, 2500° R (1390° K).

REFERENCES

1. Moffitt, Thomas P.; and Klag, Frederick W.: Analytical Investigation of Cycle Characteristics for Advanced Turboelectric Space Power Systems. NASA TN D-472, 1960.

2. Glassman, Arthur J.: Thermodynamic and Turbomachinery Concepts for Radioisotope and Reactor Brayton-Cycle Space Power Systems. NASA TN D-2968, 1965.

3. Buatti, A. U.; and Schmitt, J. W.: Design Study of a High Power In-Pile Nuclear Thermionic Space Powerplant. Rep. No. PWA-2351, Vol. 1 (NASA CR-54172), Pratt and Whitney Aircraft, July 30, 1964.

4. Ross, F. A.; and Plunkett T. F.: Conceptual Design Analysis of A 5 MWE Thermionic Reactor Space Propulsion Plant. Douglas Rep. No. SM-46275, Douglas Aircraft Co., Inc., 1965.

5. Moeckel, Wolfgang E.; Baldwin, Lionel V.; English, Robert E.; Lubarsky, Bernard; and Maslen, Stephen H.: Satellite and Space Propulsion Systems. NASA TN D-285, 1960.

6. Fiero, Ivan B.: Establishing Allowable Temperature Gradients for Tungsten - Uranium Dioxide Fuel Elements Using Experimental Cyclic Strain Data. NASA Technical Note, estimated publication date, November, 1967.

7. Paxton, H. C.; and Graves, Glen A.: Critical Masses of Fissionable Metals as Basic Nuclear Safety Data. Rep. No. LA-1958 (Del.), Los Alamos Scientific Lab., Apr. 1956, p. 8.

8. Paxton, H. C.: Los Alamos Critical-Mass Data. Rep. No. LAMS-3067, Los Alamos Scientific Lab., Apr. 1964, p. 55.

9. Barber, Clayton E.: A FORTRAN IV Two-Dimensional Discrete Angular Segmentation Transport Program. NASA TN D-3573, 1966.

10. Joanou, G. D.; and Dudek, J. S.: GAM-II. A B_3 Code for the Calculation of Fast-Neutron Spectra and Associated Multigroup Constants. Rep. No. GA-4265, General Dynamics Corp., Sept. 16, 1963.

11. Fox, Thomas A.; Mueller, Robert A.; Ford, C. Hubbard; and Alger, Donald L.: Critical Mass Studies With NASA Zero Power Reactor II. I: Clean Homogeneous Configurations. NASA TN D-3097, 1965.

12. Carpenter, S. G.; Mountford, L. A.; Springer, T. H.; and Tuttle, R. J.: Recent Results of Doppler Measurements In Fast-Neutron Spectra. Proceedings of the Conference on Safety, Fuels, and Core Design in Large Fast Power Reactors, Argonne National Lab., Illinois, October 11-14, 1965. Rep. No. ANL-7120, Argonne National Lab., 1965, pp. 614-615.

13. McCarthy, W. J., Jr.; and Okrent, D.: Fast Reactor Kinetics. Reactor Physics and Control. Vol. 1 of The Technology of Nuclear Reactor Safety. T. J. Thompson and J. G. Beckerley, eds., MIT Press, 1964, pp. 530-607.

14. Nakache, F. R.: Review and Evaluation of Temperature-Induced Feedback Mechanisms in Fast Power Reactors. Rep. No. UNC-5054, United Nuclear Corp., Apr. 1, 1963.

15. Anon.: Performance Characteristics of a Large Fast Breeder Reactor Core with Bundle Controlled Expansion (BCEX) Fuel Assemblies. Rep. No. WCAP-3589-2, Westinghouse Electric Corp., May 1966.

16. Joanow, G. D.; Smith, C. V.; and Vieweg, H. A.: GATHER-II - An IBM-7090 FORTRAN-II Program for the computation of Thermal-Neutron Spectra and Associated Multigroup Cross-Sections. Rep. No. GA-4132, General Dynamics Corp., July 8, 1963.

17. Lathrop, K. D.: DTF-IV - A FORTRAN-IV Program for Solving the Multigroup Transport Equation with Anisotropic Scattering. Rep. No. LA-3373, Los Alamos Scientific Lab., July 15, 1965.

18. Celnik, J.; and Spielberg, D.: Gamma Spectral Data for Shielding and Heating Calculations. Rep. No. UNC-5140 (NASA CR-54794), United Nuclear Corp., Nov. 30, 1965.

19. Malenfant, Richard E.: QAD: A Series of Point-Kernel General-Purpose Shielding Programs. Rep. No. LA-3573, Los Alamos Scientific Lab., Apr. 1967.

20. Caswell, Bruce F.; and Balzhiser, Richard E.: The Critical Heat Flux for Boiling Liquid Metal Systems. Chem. Eng. Progr. Symp. Ser., vol. 62, no. 64, 1966, pp. 41-46.

21. Joseph, Leon: Performance of Fuel Elements in Nuclear Power Plants. Nucleonics, vol. 24, no. 3, Mar. 1966, pp. 51-54.

22. DeMastry, John A.: Liquid Metals In Space Power Systems. Battelle Tech. Rev., vol. 15, no. 3, Mar. 1966, pp. 17-21.

23. Dwyer, O. E.: Recent Developments in Liquid-Metal Heat Transfer. At. Energy Rev., vol. 4, no. 1, 1966, pp. 3-92.

24. Magee, P. M.; and Tromel, R. H.: Heat Transfer From Fuel Elements In a Tightly Packed, Liquid-Metal-Cooled Compact Reactor. Am. Nucl. Soc. Trans., vol. 9, no. 2, Nov. 1966, pp. 569-570.

25. Lubarsky, Bernard; and Kaufman, Samuel J.: Review of Experimental Investigations of Liquid-Metal Heat Transfer. NACA TN 3336, 1956.

26. Subbotin, V. I.; Ushakov, P. A.; Kirillov, P. L.; Ibragimov, M. Kh.; Ivanovskiy, M. N.; Nomofilov, Ye, V.; and Sorokin, V. P.: Heat Transfer from Fuel Elements of Liquid Metal-Cooled Reactors. Reactor Engineering and Equipment. Vol. 8 of the Proceedings of the Third International Conference on the Peaceful Uses of Atomic Energy. United Nations, 1965, pp. 192-203.

27. Bussard, R. W.; and DeLauer, R. D.: Fundamentals of Nuclear Flight. McGraw-Hill Book Co., Inc., 1965.

28. Sparrow, E. M.: Temperature Distribution in an Internally Cooled, Heat-Generating Solid. Paper No. 60-SA-15, ASME, June 1960.

29. Den Hartog, Jacob P.: Advanced Strength of Materials. McGraw-Hill Book Co., Inc., 1952, p. 106.

30. Miller, John V.: Estimating Thermal Conductivity of Cermet Fuel Material for Nuclear Reactor Application. NASA TN D-3898, 1967.

NASA-Langley, 1968 —— 22 E-3936